



# VCU

Virginia Commonwealth University  
VCU Scholars Compass

---

Theses and Dissertations

Graduate School

---

2015

## Characterization of the Interactions between Staphylococcal Phage 80 Alpha Scaffold and Capsid Proteins

Laura Klenow  
*Virginia Commonwealth University*

Follow this and additional works at: <https://scholarscompass.vcu.edu/etd>

 Part of the [Molecular Genetics Commons](#), [Pathogenic Microbiology Commons](#), and the [Virology Commons](#)

© The Author

---

Downloaded from

<https://scholarscompass.vcu.edu/etd/3917>

This Thesis is brought to you for free and open access by the Graduate School at VCU Scholars Compass. It has been accepted for inclusion in Theses and Dissertations by an authorized administrator of VCU Scholars Compass. For more information, please contact [libcompass@vcu.edu](mailto:libcompass@vcu.edu).

© Laura Ann Klenow 2015

All Rights Reserved

CHARACTERIZATION OF THE INTERACTIONS BETWEEN  
STAPHYLOCOCCAL PHAGE 80 ALPHA SCAFFOLD AND CAPSID PROTEINS

A thesis submitted in partial fulfillment of the requirements for the degree of Master of  
Science at Virginia Commonwealth University

by

LAURA ANN KLENOW  
B.S., Virginia Polytechnic Institute and State University, 2008

Director: Gail E. Christie, Ph.D.  
Professor, Department of Microbiology and Immunology  
Virginia Commonwealth University  
Richmond, Virginia

Virginia Commonwealth University  
Richmond, Virginia  
May 2015

## Acknowledgement

I would like to extend my deepest gratitude to my mentor, Dr. Gail Christie. Thank you so much for pushing me to be a better scientist and researcher. The skills I have learned from working with you and watching how you attack new challenges will serve me for the rest of my career. To my committee members, Dr. Michael McVoy, and Dr. Darrell Peterson, thank you for all of your helpful comments and ideas that have helped guide my project towards a cohesive finish. I would also like to thank all the Christie Lab members, past and present, for all of your help on projects, presentations, and on special occasions, just making it through the day. Finally, I would like to sincerely thank all of the members of the Jefferson and Cornelissen labs for being a wonderful support system not only in lab, but outside of it as well.

## Dedication

To my amazing husband Brad. When I first told you that I wanted to quit my job and go back to school, you took it in stride. When I told you that I had been accepted at a school in another city and we would be separated for two years, your support never wavered. I am so thankful for all of your patience and understanding these past years, I couldn't have done it without you.

## Table of Contents

	Page
Acknowledgements.....	ii
Dedication.....	iii
List of tables.....	vi
List of figures.....	vii
List of abbreviations.....	ix
Abstract.....	xii
Chapter	
1 Introduction.....	1
<i>Staphylococcus aureus</i> virulence and mobile genetic elements.....	1
Bacteriophage 80 $\alpha$ and the molecular pirate SaPI1.....	2
SaPI1 mobilization via helper phage 80 $\alpha$ .....	7
Phage 80 $\alpha$ capsid assembly and its interaction with two alternative scaffolds.....	7
2 Materials and Methods.....	9
3 Investigation of the interaction between 80 $\alpha$ scaffold and major capsid proteins.....	26
Introduction.....	26
Compensatory 80 $\alpha$ capsid mutations.....	27
Effect of C-terminal scaffold mutations on SaPI1.....	31

	Identifying the specific scaffold and capsid interface.....	31
	Discussion.....	35
4	The role of N-terminal cleavage of scaffold and major capsid proteins in staphylococcal phage 80 $\alpha$ and SaPI1.....	39
	Introduction.....	39
	N-terminal cleavage of scaffold.....	40
	Effect of scaffold mutations on SaPI1.....	40
	Effect of uncleavable capsid on 80 $\alpha$ growth.....	44
	Discussion.....	44
5	Discussion.....	49
	References.....	56
	Vita.....	60

## List of Tables

	Page
Table 1: Bacterial strains used in this study.....	10
Table 2: Plasmids used in this study.....	12
Table 3: Primers used in this study.....	14

## List of Figures

	Page
Figure 1: Schematic of 80 $\alpha$ capsid assembly and the SaPI1 CpmA and CpmB redirection of 80 $\alpha$ capsid assembly.....	4
Figure 2: Model for high frequency SaPI1 transduction.....	6
Figure 3: Alignment of the C-termini of SaPI1 CpmB and 80 $\alpha$ gp46.....	28
Figure 4: Representative effect of gp46 I203T mutation on 80 $\alpha$ phage titer.....	30
Figure 5: Predicted secondary structure of hypothesized alpha-helical interaction site between gp46 (scaffold protein) and gp47 (major capsid protein).....	33
Figure 6: Schematic of the proposed salt-bridge interaction between R202 in gp46 and either E50 or E53 in gp47.....	34
Figure 7: Effect of E50R and E53R gp47 major capsid protein mutations on 80 $\alpha$ phage titer.....	36
Figure 8: Effect of E50R and E53R gp47 major capsid protein mutations paired with an R202E gp46 scaffold mutation on 80 $\alpha$ phage titer.....	37
Figure 9: Effect of N-terminally cleaved scaffold on 80 $\alpha$ titer.....	41
Figure 10: Electron micrographs of CaCl purified phage structures from scaffold mutants.....	42
Figure 11: Effect of uncleavable capsid protein, gp47, on 80 $\alpha$ phage titer.....	45

Figure 12: Cryo-EM of capsid formation in wild-type 80 $\alpha$  and uncleavable capsid (gp47 F14A).....46

Figure 13: I-TASSER model of gp46 modeled onto the HK97-fold.....52

## List of Abbreviations

A	Adenine
a.a.	amino acid
BHI	brain heart infusion
bp	base pair
C	cytosine
CaCl <sub>2</sub>	calcium chloride
CFU	colony forming unit
cm	centimeter
CY-GL	casamino acids yeast extract glycerophosphate
DNA	deoxyribonucleic acid
dNTP	deoxynucleotide triphosphate
E	glutamic acid
<i>E. coli</i>	<i>Escherichia coli</i>
g	gram
G	guanine
GL	beta-glycerophosphate disodium salt pentahydrate
I	isoleucine
K	lysine
Klett	Klett-Summerson units

L	liter
LB	Luria-Bertani
M	methionine
M	molar
MC	mitomycin C
ml	milliliter
mM	millimolar
MOI	multiplicity of infection
ms	millisecond
MW	molecular weight
NaCl	sodium chloride
OD	optical density
PCR	polymerase chain reaction
PFU	plaque forming unit
rpm	revolutions per minute
R	arginine
RT	room temperature
<i>S. aureus</i>	<i>Staphylococcus aureus</i>
SaPI	<i>Staphylococcus aureus</i> pathogenicity island
SOS	Save Our Ship, cellular response to DNA damage
TAE	Tris-acetate-EDTA
TSA	tryptic soy agar
TSB	tryptic soy broth

TU	transducing unit
μg	microgram
μl	microliter
μm	micrometer
μM	micromolar
UV	ultraviolet light
vol/vol	volume to volume
wt/vol	weight to volume
X	times
Xgal	5-bromo-4-chloro-3-indoyl-B-D-galactopyranside

## Abstract

# CHARACTERIZATION OF THE INTERACTIONS BETWEEN STAPHYLOCOCCAL PHAGE 80 ALPHA SCAFFOLD AND CAPSID PROTEINS

By Laura Ann Klenow

A thesis submitted in partial fulfillment of the requirement for the degree of Master of Science at Virginia Commonwealth University.

Virginia Commonwealth University, 2015

Major Director: Gail E. Christie, Ph.D.

Professor, Department of Microbiology and Immunology

Staphylococcal phage 80 $\alpha$  can serve as a helper bacteriophage for a family of mobile genetic elements called *Staphylococcus aureus* pathogenicity islands (SaPIs). The prototype island, SaPI1, is able to hijack the 80 $\alpha$  capsid assembly process and redirect capsid formation to yield smaller, phage-like transducing particles carrying SaPI DNA. Capsid size redirection is accomplished through two SaPI1-encoded gene products, CpmA and an alternate scaffold protein, CpmB. The normal 80 $\alpha$  scaffold and the SaPI1 CpmB scaffold share a small block of conserved residues at their C-termini, several of which had been shown to be essential for CpmB function. This led to the hypothesis that

the C-termini of both the phage and SaPI scaffolds interact in similar ways with the major capsid protein. The goal of this study was to test this hypothesis and to identify the amino acid residues at the capsid-scaffold interface, using a genetic approach.

## Chapter 1

### Introduction

#### *Staphylococcus aureus* virulence and mobile genetic elements

*Staphylococcus aureus* is a widespread Gram-positive bacterium that is commonly found as a normal inhabitant of human skin and the mucosal epithelia. It is estimated that 20% of individuals' anterior nares are persistently colonized, with approximately 30% of the population intermittently colonized (Gordon et al., 2008). While *S. aureus* is generally a commensal bacterium, it is in possession of a vast array of virulence factors and toxins that are capable of causing an assortment of systemic and local infections (Xia et al., 2013). Antibiotic resistance in *S. aureus* arose two years after the introduction of methicillin and has been increasing in prevalence in the clinical setting since that time (Jevons, 1961). Nosocomial *S. aureus* infections are the second most reported hospital acquired infections and while the majority of resistant strains were reported in clinical settings, community acquired (CA)-MRSA cases, or incidents where the persons infected had no prior hospitalizations, are on the rise as well (Archer, 2008; Knox et al. 2015; Lowy, 2003).

While antibiotic resistance is a valid concern, the pathogenicity of *S. aureus* ranges from causing local skin abscesses all the way to disseminated septic shock, due in large part to a host of over 20 known virulence factors (Archer, 1998). Virulence factors can be

acquired through the highly promiscuous nature of bacterial horizontal gene transfer (HGT). HGT is accomplished through a variety of mechanisms, as virulence genes and toxins are often carried by mobile genetic elements (MGEs) such as bacteriophages, pathogenicity islands, and plasmids (Novick, 2003). Along these lines, *S. aureus* can be parasitized by staphylococcal phage 80 $\alpha$ , which on its own is able to transfer chromosomal and plasmid-encoded genes through generalized transduction (Dyer et al. 1985). However, adding another layer of complexity to the issue is the fact that 80 $\alpha$  can also mediate specific high-frequency transduction of *Staphylococcus aureus* pathogenicity islands (SaPIs) which also carry genes for several virulence factors, such as the toxic shock syndrome toxin (Novick, 2003).

#### Bacteriophage 80 $\alpha$ and the molecular pirate SaPI1

Staphylococcal bacteriophage 80 $\alpha$  is a temperate, double-stranded DNA (dsDNA) phage of the family *Siphoviridae* (Christie et al., 2010). The mature 80 $\alpha$  virion has a 63 nm diameter, icosahedral capsid with T=7 symmetry. Attached to the capsid is a 190 nm long non-contractile, flexuous tail with an elaborate baseplate that is studded with six tail fibers (Spilman et al., 2011). 80 $\alpha$  is a temperate bacteriophage, meaning that it can reside as a stable lysogen integrated into the host staphylococcal chromosome, or alternatively infect the cell and cause lysis after a productive phage infection (Christie et al., 2010).

Most dsDNA, tailed bacteriophages replicate in a similar manner. After infecting a cell and shutting down certain host cell macromolecular synthesis processes in favor of preferentially producing phage components, a small, empty prohead structure is formed by the aggregation of scaffold-chaperoned capsid proteins (Rossman, 2013). Later in the

assembly process, the genome is packaged through the portal into the procapsid. DNA packaging is an energy consuming process and is powered by the small and large subunits of terminase, which are ATP dependent (Rossman, 2013). While the genome is packaged, the internal scaffolding protein exits and the procapsid expands to a larger, DNA-filled mature capsid (Prevelige et al., 2012).

The staphylococcal phage 80 $\alpha$  follows a similar pathway (Figure 1). The 80 $\alpha$  capsid assembly pathway involves formation of an empty, transient procapsid composed of 415 copies of the major capsid protein, gene product (gp) 47; 100-200 copies of the scaffold protein, gp46; a portal protein, gp42; and approximately 20 copies of an uncharacterized minor capsid protein, gp44 (Tallent et al., 2007; Poliakov et al., 2008). Like other tailed dsDNA bacteriophages, the capsid protein of 80 $\alpha$  shows a conformation similar to that first described in phage HK97, the so-called HK97 fold (Johnson, 2010). During procapsid assembly, scaffold protein gp46 serves as a chaperone for the aggregation of major capsid protein gp47. Both gp46 and gp47 are N-terminally cleaved by 13 and 14 residues, respectively, between phenylalanine and alanine residues within a conserved amino acid sequence motif (Poliakov et al., 2008). This cleavage is carried out by a host-encoded cysteine protease, phage-related ribosomal protease (Prp) (Wall et al., 2015). Procapsid expansion and maturation is dependent upon a conformational change involving a proline at residue 132 (P132) in gp47 (Spilman et al., 2011). 80 $\alpha$  procapsid expansion involves dynamic remodeling of the surface gp47 proteins due to the rotational effects of P132 altering its angle in the spine helix of capsid, resulting in an expansion that roughly doubles the volume of the procapsid (Spilman et al., 2011). Procapsid expansion occurs simultaneously with the release of gp46, and the headful

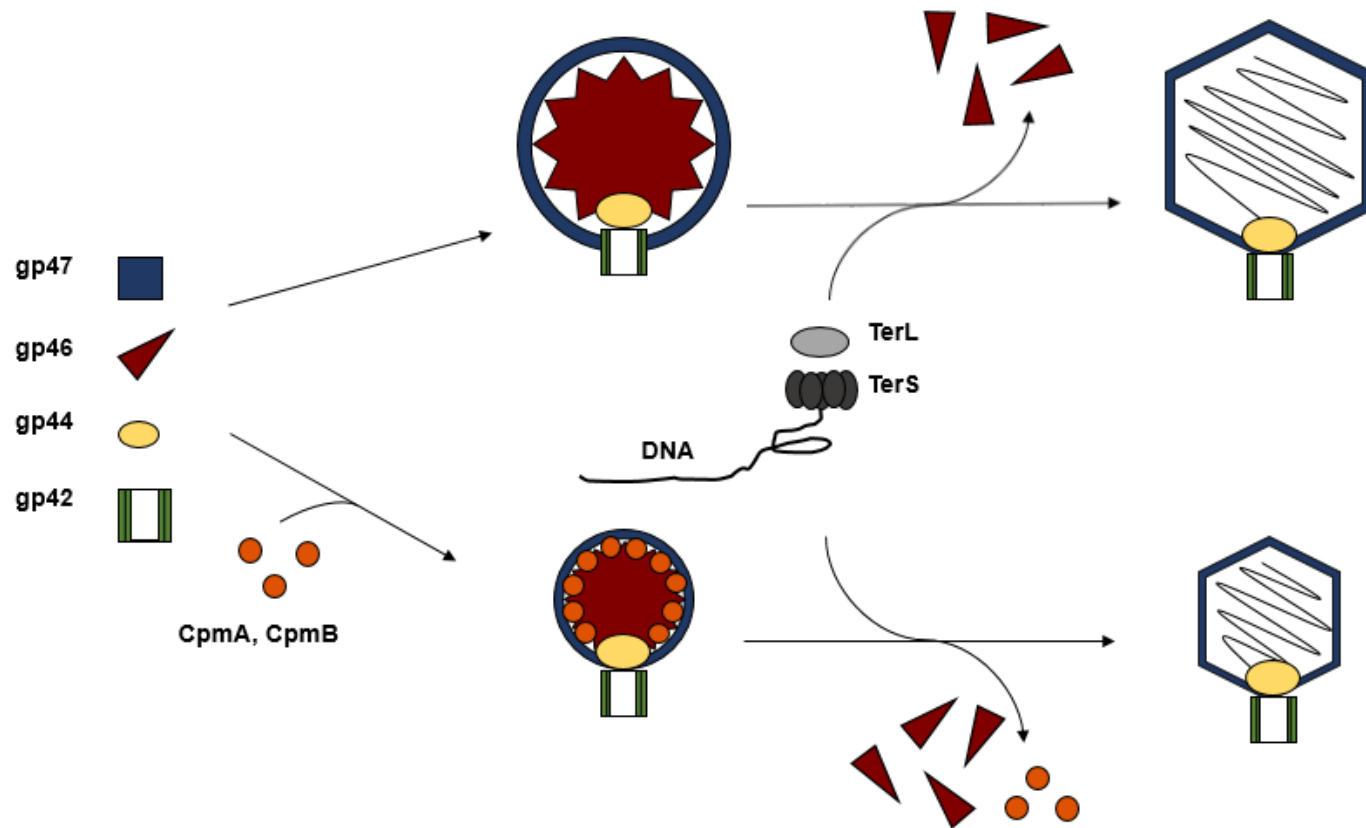


**Figure 1: Schematic of 80 $\alpha$  capsid assembly and the SaPI1 CpmA and CpmB redirection of 80 $\alpha$  capsid assembly.**

80 $\alpha$  scaffolding protein, gp46, serves as a chaperone for the proper aggregation of major capsid protein, gp47. Upon DNA packaging, the procapsid expands to form a mature virion. In the presence of the SaPI1 encoded CpmA and CpmB capsid size redirection genes, SaPI1 forms a smaller procapsid, resulting in a transducing particle that is approximately one-third the volume of the mature 80 $\alpha$  virion.

packaging of the dsDNA genome by the small (gp40, TerS) and large (gp41, TerL) terminase subunits, resulting in a mature capsid (Spilman et al., 2011). Following capsid maturation, the non-contractile tail attaches to the capsid via gp42 resulting in a mature, viable virion.

However, instead of one possible outcome, the mature viable phage virion, there is a second route of capsid assembly possible. Phage 80 $\alpha$  also serves as a “helper” phage that aids in the mobilization of several SaPIs. SaPIs are a class of MGEs, roughly 14-27 kb in size, that stably integrate into the host chromosome and often carry antibiotic resistance and toxin genes (Novick et al., 2010). SaPIs are considered molecular pirates because they package their own genomes into transducing particles comprised of helper phage-encoded proteins. One striking feature of this appropriation of the helper phage by a SaPI is redirection of the capsid assembly process to construct T=4 capsids with one-third the volume of the mature 80 $\alpha$  capsid (Christie et al., 2012). This difference in capsid size directly parallels the disparity between the genome sizes of 80 $\alpha$  (~44 kb) and the prototypical pathogenicity island used in this work, SaPI1 (~15 kb). While SaPI1 can package its genome into either a small or large capsid, 80 $\alpha$  is unable to package its complete genome into the smaller SaPI1 transducing particle. Furthermore, SaPI1 preferentially packages its own genome using a SaPI1-encoded small terminase subunit (Ubeda et al., 2009). This results in interference with helper phage propagation and the efficient assembly of SaPI1 transducing particles from the phage structural proteins (Figure 2).

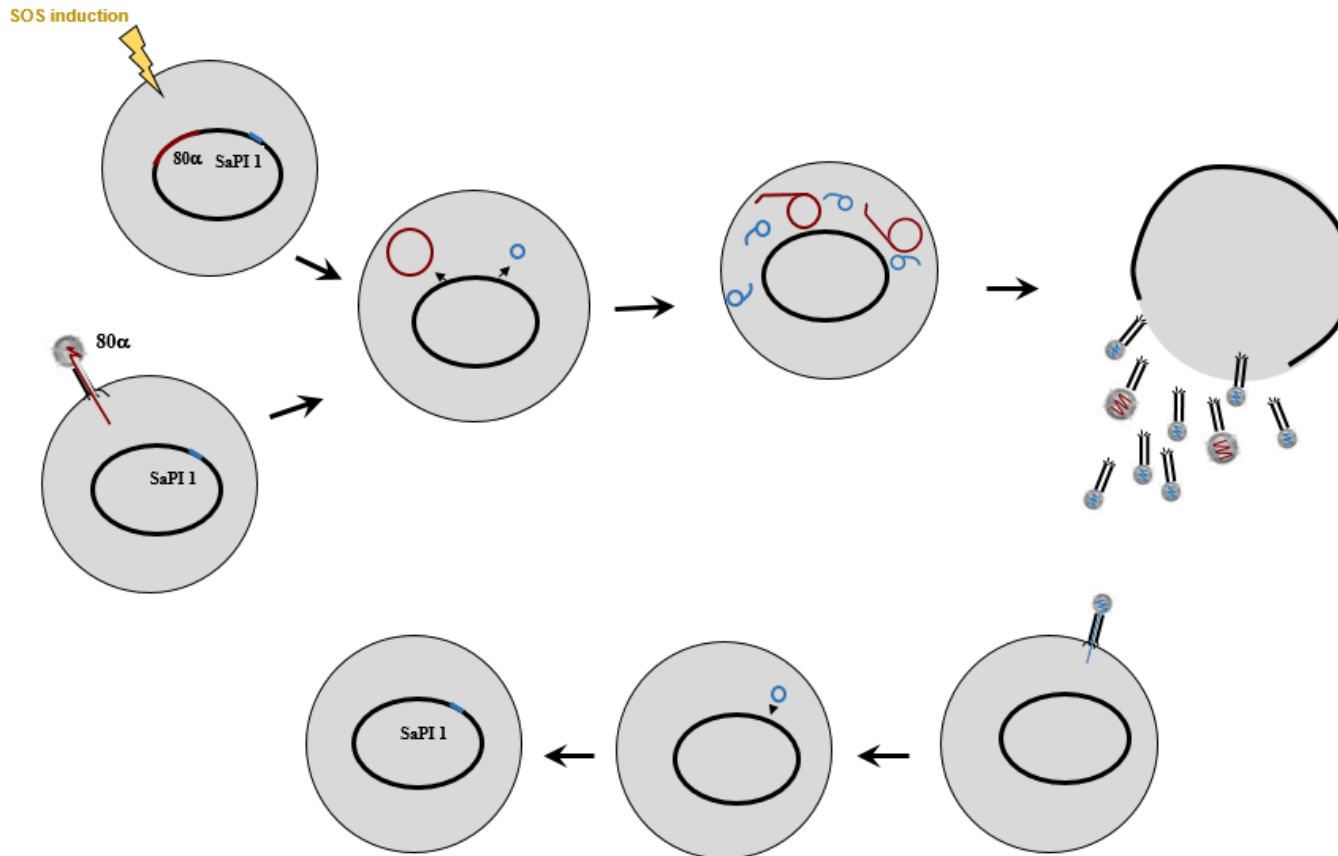


**Figure 2: Model for high frequency SaPI1 transduction**

Following phage infection or the induction of a lysogenic prophage, SaPI1 excises from the *S. aureus* chromosome, re-circularizes and begins replicating, packaging its DNA preferentially in small capsids. Upon lysis, progeny phage and SaPI1 transducing particles are released, and are able to propagate throughout *S. aureus*, infecting naïve cells.

### SaPI1 mobilization via helper phage 80α

Upon infection by 80α or the induction of an 80α prophage from the host cell chromosome by the SOS response, a phage-encoded anti-repressor, Sri inhibits the SaPI1 repressor, StI (Tormo-Mas et al., 2010). The SOS response is a global cellular response that is activated when DNA damage is so widespread that normal DNA repair mechanisms are ineffective (Willey, 2014). This derepression results in expression of SaPI1 genes leading to excision of SaPI1 from the host chromosome and its subsequent replication. With such a small genome, it is not surprising that SaPIs rely heavily on 80α for transducing particle assembly. Due to this ability to redirect capsid assembly, there is usually a one-hundred fold reduction in phage titer when there is also a SaPI present in the host cell. The completed SaPI1 transducing particles are now able to infect other naïve host cells upon lysis, potentially transferring virulence or toxin genes to the surrounding bacterial population (Figure 2).

### Phage 80α capsid assembly and its interaction with alternative scaffolds

Capsid assembly is an essential process in the formation of mature 80α virions and SaPI1 transducing particles. As previously discussed, phage 80α capsid assembly begins with the gp46 scaffold acting as a chaperone protein for gp47 (Dokland, 1999). The 80α procapsid is formed from multiple copies of gp46, gp47, the portal protein gp42, and the minor capsid protein gp44. Prior to, or concurrently with procapsid expansion and DNA packaging, the gp46 scaffolding proteins are lost. In the presence of SaPI1, the 80α capsid protein gp47 interacts with the SaPI1-encoded alternate scaffold, CpmB or gp6 (Dearborn et al., 2011). A second SaPI encoded gene, *cpmA* or gp7, is also involved in

forming small capsids, but its role is not well understood. The internal structures of 80 $\alpha$  and SaPI1 procapsids are significantly different. Cryo-EM reconstructions of the procapsids revealed finger-like projections that extend towards the center of the procapsid of SaPI1 which were completely absent in 80 $\alpha$ . Previous studies have shown that these finger-like densities are consistent with CpmB, the alternate scaffold protein, which forms a scaffold-like dimer that then associates with phage capsid (Dearborn et al., 2011). The interaction between 80 $\alpha$  capsid with two alternative scaffolds, the native phage scaffold protein and the alternate scaffold produced by SaPI1, is a unique feature of the system.

The specific interactions between capsid and these two different scaffolding proteins are not well understood at this time. Previous work in our lab suggests that the C-terminus of SaPI1 scaffold is involved in the interaction with the phage capsid protein (E.A. Wall, unpublished). Similarities between the C-terminus of the phage and SaPI1 scaffold proteins suggest that both scaffold proteins interact with major capsid protein gp47 in a similar manner.

The goal of this study was to investigate the residues involved in the 80 $\alpha$  scaffold:capsid interface and determine whether these interactions were shared with the phage capsid and SaPI1 scaffold. Secondly, the role of N-terminal proteolytic cleavage of gp46 and gp47 in assembly of phage capsids and SaPI1 transducing particles was explored.

## Chapter 2

### Materials and Methods

Note: All reagents used in this work were acquired through major suppliers including Fisher Scientific (Waltham, MA), and Sigma-Aldrich (St. Louis, MO), unless indicated otherwise.

#### 2.1 Bacterial Culture

All bacterial strains used in this work are listed in Table 1. *S. aureus* cultures were grown overnight in Luria-Bertani (LB) broth (Fisher Scientific, Waltham, MA), or Tryptic Soy Broth (TSB) (Fisher Scientific, Waltham, MA). All broth cultures were incubated at 37°C on an orbital shaker at 200 rpm. *S. aureus* cultures were also grown on LB agar plates (1.8% agarose) and Tryptic Soy Agar (TSA) plates (1.8% agarose) and incubated overnight at 30°C. When necessary, the media was supplemented with erythromycin (5 µg/ml). *S. aureus* strains carrying 80α prophage were plated on beta-glycerophosphate disodium salt pentahydrate (GL) agar (Novick, 1991) and incubated overnight at 30°C.

*Escherichia coli* strains were incubated overnight at 37°C on either LB or TSA plates, in addition to being grown in LB broth or TSB. Media for use with *E. coli* strains was supplemented with ampicillin (100 µg/ml) when needed.

**Table 1: Bacterial strains used in this study**

<b><i>S. aureus</i> Strains</b>	<b>Background</b>	<b>Integrated Prophage/SaPI</b>	<b>Reference</b>
RN4220	4220	None	Kreiswirth, B.N., <i>et al.</i> , 1983.
RN10616	4220	80 $\alpha$	Ubeda, C., <i>et al.</i> , 2009.
RN10628	4220	80 $\alpha$ SaPI1 <i>tst::tetM</i>	Ubeda, C., <i>et al.</i> , 2009.
ST91	4220	80 $\alpha$ $\Delta$ gp46	Lab strain
ST247	4220	80 $\alpha$ gp46 $\Delta$ 2-13	Lab strain
ST248	4220	80 $\alpha$ $\Delta$ gp47	Lab strain
ST278	4220	80 $\alpha$ gp46 R202S	Lab strain
ST279	4220	80 $\alpha$ gp46 R202E	Lab strain
ST358	4220	80 $\alpha$ gp46 I203T	This study
ST361	4220	80 $\alpha$ gp47 F14A	This study
ST365	4220	ST247 + SaPI1	This study
ST366	4220	ST278 + SaPI1	This study
ST367	4220	ST279 + SaPI1	This study
ST368	4220	ST358 + SaPI1	This study
ST375	4220	80 $\alpha$ gp47 E50R	This study
ST376	4220	80 $\alpha$ gp47 E53R	This study
ST377	4220	80 $\alpha$ gp46 R202E + gp47 E50R	This study
ST378	4220	80 $\alpha$ gp46 R202E + gp47 E53R	This study
<b><i>E. coli</i> Strain</b>	<b>Description</b>		<b>Source</b>
Stellar™ Competent Cells	HST08 derivative, high transformation efficiency strain. <i>E. coli</i> F <sup>-</sup> , <i>endA1</i> , <i>supE44</i> , <i>thi-1</i> , <i>recA1</i> , <i>relA1</i> , <i>gyrA96</i> , <i>phoA</i> , $\Phi$ 80d <i>lacZ</i> $\Delta$ M15, $\Delta$ ( <i>lacZYA-argF</i> )U169, $\Delta$ ( <i>mrr-hsdRMS-mcrBC</i> ), $\Delta$ <i>mcrA</i> , $\lambda$ <sup>-</sup>		Clontech

## 2.2 DNA Manipulations: Plasmid Construction

All plasmids used or created for this work are listed in Table 2. Restriction endonucleases, restriction enzyme buffers, and bovine serum albumin (BSA) used for DNA manipulations were purchased from New England Biolabs (Ipswich, MA) and were used in accordance with the manufacturer's instructions. Restriction digests were performed in a volume of 25  $\mu$ l, or multiples thereof, depending upon the downstream application(s) of the DNA product(s). Plasmid construction was accomplished through polymerase chain reaction (PCR) amplification of the desired insert, vector preparation (including PCR purification, restriction enzyme digestion, and gel extraction), In-Fusion reaction and finally confirmation of the construct through Sanger sequencing. Plasmid DNA preparations were performed using the QIAprep®Spin Miniprep Kit (Qiagen; Valencia, CA) in accordance with the manufacturer's instructions. Plasmid DNA was eluted in warmed (65°C) HPLC-grade water for DNA sequencing. All PCR products were analyzed and/or prepared for PCR purification using agarose gel electrophoresis. PCR products were purified using the QIAquick PCR Purification Kit (Qiagen; Valencia, CA) and gel extractions were performed using the Nucleospin® Gel and PCR Clean-up Kit (Macherey-Nagel; Düren, Germany) in accordance with the manufacturer's instructions. All DNA concentrations were determined using a Nanodrop 1000 spectrophotometer (Thermo Scientific; Waltham, MA). The Infusion® HD cloning kit (Clontech; Mountain View, CA), which utilizes the Gibson assembly method (Gibson, 2011), was used instead of an insert-vector ligation in accordance with the manufacturer's instructions. All plasmids were verified by Sanger sequencing through Eurofins MWG Operon.

**Table 2: Plasmids created or used for this this study**

<b>Plasmid</b>	<b>Description</b>	<b>Reference</b>
pLAK1	pMAD derivative with 80 $\alpha$ gp46 mutation I203T	This study
pLAK2	pMAD derivative with 80 $\alpha$ gp47 mutation E50R	This study
pLAK3	pMAD derivative with 80 $\alpha$ gp47 mutation E53R	This study
pLAK4	pMAD derivative with 80 $\alpha$ gp46 mutation R202E and gp47 mutation E50R	This study
pLAK5	pMAD derivative with 80 $\alpha$ gp46 mutation R202E and gp47 mutation E53R	This study
pMAD	Shuttle vector used for allelic exchange in Gram-positive bacteria	Arnaud <i>et al.</i> , 2004
pMED2	pMAD derivative with 80 $\alpha$ gp47 mutation F14A	Lab Strain

### 2.3 Polymerase Chain Reaction (PCR)

PCR reactions were performed using a T-Gradient Thermoblock thermocycler (Biometra; Gottingen, Germany). Primers listed in Table 3 were obtained from Integrated DNA Technologies (Coralville, IA). The lyophilized primers were reconstituted with HPLC-grade water to a final concentration of 1 mM. Primer working stock aliquots were prepared by 1:100 dilution with HPLC-grade water to 10  $\mu$ M. All inserts were amplified using *PfuUltra* II Fusion HS DNA Polymerase (Agilent Technologies; Santa Clara, CA) in the following manner: 1x *PfuUltra* II reaction buffer (Agilent Technologies; Santa Clara, CA), 100  $\mu$ M dNTPs (Invitrogen; Grand Island, NY), 5-30 ng vector DNA input template, 0.2  $\mu$ M of both the forward and reverse primers, and 0.5  $\mu$ l of *PfuUltra* II Fusion HS DNA polymerase, and brought to a final reaction volume of 50  $\mu$ l. All PCR reaction master mixes were scaled up as needed with 10% excess to account for pipetting error. The following PCR parameters were followed for targets <10 kb: initial denaturation for 2 minutes at 95°C, followed by 34 cycles of denaturation for 20 seconds at 95°C, primer annealing for 15 seconds, and primer extension for 15 seconds per kb of target DNA at 72°C. A final 3 minute primer extension step was performed at 72°C. All reactions were kept at 4°C following the final extension prior to being stored at -20°C. Annealing temperatures for each primer were optimized based on the melting temperature ( $T_m$ ) of each primer, as shown in Table 3, and were generally the average  $T_m$ -5°C.

Colony PCR was performed by preparing the DNA template as follows: 1 isogenic colony was picked and smeared in an even layer into a sterile PCR tube,

**Table 3: Primers used in this study**

Primer	Sequence (5'-3')	Direction	T <sub>m</sub> (°C)	DNA Template
<b>Plasmid Construction Primers</b>				
<b>pLAK1</b>				
EAW5	<u>CGATGCATGCCATGG</u> * <u>TGGTCGAAAA</u> <u>CAAGGACTTTAGCGATAG</u>	F	58.6	RN10616
EAW159	<u>TTTAAT(CG)TTCTTTT</u> * <u>TTGTCTAGCTA</u> <u>TTTCAGCTAAGTTTTGCG</u>	R	59.3	RN10616
EAW8	<u>GGCGATATCGGATCC</u> * <u>TTCCAATGAT</u> <u>TTCGGGCATGTTAC</u>	R	56.0	RN10616
EAW160	<u>AAAAGAA(CG)ATTAAA</u> * <u>AATTAACGGA</u> <u>GGCATTAAATGGAACAAAC</u>	F	57.6	RN10616
<b>pLAK2</b>				
EAW58	<u>CGATGCATGCCATGG</u> * <u>TTAATAGCTA</u> <u>GCACTTAATTGTGTTGGC</u>	F	55.8	RN10616
EAW171	<u>CATAAC(ACG)TTGTAA</u> * <u>GATGGGCGT</u> <u>TGTGAATTCATTC</u>	R	57.9	RN10616
EAW61	<u>GGCGATATCGGATCC</u> * <u>ATATCTCAAA</u> <u>AGAACACAGCCCTTCC</u>	R	57.0	RN10616
EAW172	<u>TTACAA(CGT)GTTATG</u> * <u>GAAAACCTCTA</u> <u>AAATTATGCAATTAGGTAAGTACG</u>	F	57.9	RN10616
<b>pLAK3</b>				
EAW58	<u>CGATGCATGCCATGG</u> * <u>TTAATAGCTA</u> <u>GCACTTAATTGTGTTGGC</u>	F	55.8	RN10616
EAW173	<u>AGAGTT(ACG)CATAAC</u> * <u>CTCTTGTAAG</u> <u>ATGGGCGTTG</u>	R	59.3	RN10616
EAW61	<u>GGCGATATCGGATCC</u> * <u>ATATCTCAAA</u> <u>AGAACACAGCCCTTCC</u>	R	57.0	RN10616
EAW174	<u>GTTATG(CGT)AACTCT</u> * <u>AAAATTATGC</u> <u>AATTAGGTAAGTACGAACC</u>	F	57.2	RN10616
<b>pLAK4</b>				
EAW58	<u>CGATGCATGCCATGG</u> * <u>TTAATAGCTA</u> <u>GCACTTAATTGTGTTGGC</u>	F	55.8	ST279
EAW171	<u>CATAAC(ACG)TTGTAA</u> * <u>GATGGGCGT</u> <u>TGTGAATTCATTC</u>	R	57.9	ST279
EAW61	<u>GGCGATATCGGATCC</u> * <u>ATATCTCAAA</u> <u>AGAACACAGCCCTTCC</u>	R	57.0	ST279
EAW172	<u>TTACAA(CGT)GTTATG</u> * <u>GAAAACCTCTA</u> <u>AAATTATGCAATTAGGTAAGTACG</u>	F	57.9	ST279
<b>pLAK5</b>				
EAW58	<u>CGATGCATGCCATGG</u> * <u>TTAATAGCTA</u> <u>GCACTTAATTGTGTTGGC</u>	F	55.8	ST279
EAW173	<u>AGAGTT(ACG)CATAAC</u> * <u>CTCTTGTAAG</u> <u>ATGGGCGTTG</u>	R	59.3	ST279

**Table 3 (continued): Primers used in this study**

Primer	Sequence (5'-3')	Direction	T <sub>m</sub> (°C)	DNA Template
<b>Plasmid Construction Primers</b>				
<b>pLAK5</b>				
EAW61	<u>GGCGATATCGGATCC</u> *ATATCTCAA AGAACACAGCCCTTCC	R	57.0	ST279
EAW174	GTTATG(CGT)AACTCT*AAAATTATGC <u>AATTAGGTAAGTACGAACC</u>	F	57.2	ST279
<b>Sequencing primers</b>				
Primer	Sequence (5'-3')	Direction	T <sub>m</sub> (°C)	Template
<b>pLAK1</b>				
EAW1	<u>GTCGTTTCAGATTGCGCTTTACTACC</u>	F	57.9	pLAK1
EAW26	<u>AGTTGATTCATCAGATGAGGTTGTC</u>	F	54.9	pLAK1
PKD101	GGTAGCTAGCAGACTATAAATGGAG GTATATCTCATGGAAG	F	56.1	pLAK1
pMADSF	<u>CTAGCTAATGTTACGTTACACATTAAC</u> TAG AC	F	55.3	pLAK1
pMADSR	<u>CCCTGATGGTCGTCATCTACCTG</u>	R	58.7	pLAK1
<b>pLAK2/pLAK3/pLAK4/pLAK5</b>				
EAW1	<u>GTCGTTTCAGATTGCGCTTTACTACC</u>	F	57.9	pLAK2/pLAK3 pLAK4/pLAK5
EAW24	<u>ACG AAG ATG GCA CAC CTG</u>	F	55.2	pLAK2/pLAK3 pLAK4/pLAK5
EAW26	<u>AGTTGATTCATCAGATGAGGTTGTC</u>	F	54.9	pLAK2/pLAK3 pLAK4/pLAK5
EAW172	TTACAA(CGT)GTTATG*GAAAACCTCA <u>AAATTATGCAATTAGGTAAGTACG</u>	F	57.9	pLAK2/pLAK3 pLAK4/pLAK5
SMT46	<u>AAAAGGAAGGGCTGTGTTC</u>	F	57.0	pLAK2/pLAK3 pLAK4/pLAK5
<b>ST247</b>				
EAW6	AATAATT(T)TTTTTTG*TCTAGCTATTT <u>CAGCTAAGTTTTGCG</u>	R	58.1	ST247
EAW7	CAAAAA(A)AATTATT*AAAAATTAAC <u>GGAGGCATTTAAATGGAAC</u>	F	56.1	ST247
EAW24	<u>ACG AAG ATG GCA CAC CTG</u>	F	55.2	ST247
<b>ST361</b>				
EAW24	<u>ACG AAG ATG GCA CAC CTG</u>	F	55.2	ST361
GC47FA3	TGCGAGTAACAATGTTAAACCGCAAG T	F	59.2	ST361
PKD47	AGAATGAGTTAAAGCGAGATGTGAAA AGCGGTGATTGATTTAAAAGTAAAGT TT	F	57.3	ST361

**Annealing sequence is underlined. T<sub>m</sub> corresponds to annealing sequence. Restriction cuts marked with asterisk. Mutations in parentheses (XXX).**

microwaved, cap open, on “High” for 90 seconds, and thoroughly vortexed with 10  $\mu$ l of HPLC grade water.

#### 2.4 Agarose Gel Electrophoresis

Analytical and preparatory agarose gels were prepared to assess if PCR reactions were successful, prepare enzymatic restriction digests for gel purification, and to verify insertions or deletions of gene products in vectors. 0.6% and 1% agarose (KSE Scientific; Durham, NC) gels were prepared with 1X Tris-acetate-EDTA (TAE) buffer and 0.3  $\mu$ g/ml ethidium bromide.

Samples for analytical gels were prepared in the following manner: 1  $\mu$ l of 6X loading dye (50% v/v glycerol, 50% v/v 1X TAE, bromophenol blue added to desired color) was thoroughly mixed with 2  $\mu$ l of the appropriate ladder, either Hyperladder I or Hyperladder IV (both supplied by Biorline; Taunton, MA). 1  $\mu$ l of 6X loading dye was thoroughly mixed with 2  $\mu$ l of sample to be analyzed and loaded into 1% agarose gels and electrophoresed in 1X TAE buffer at 115V for approximately 50 minutes, or until ladder bands were easily visualized.

Samples for preparatory gels were prepared in the following manner: 1  $\mu$ l of 6X loading dye was thoroughly mixed with 2  $\mu$ l of the appropriate ladder, either Hyperladder I or Hyperladder IV. For larger volumes, the loading dye was scaled up as follows: 25  $\mu$ l 6X loading dye was added to 150  $\mu$ l PCR reactions or enzymatic restriction digests. For gel purifications, the entire sample plus the appropriate amount of loading dye was loaded into a single, large lane on the gel and electrophoresed in 1X TAE at 115V until ladder bands were easily visualized.

Following electrophoresis, all gels were examined on a White/UV transilluminator (VWR; Randor, PA) and photographed using a Fotodyne FOTO/Analyst Apprentice - UV system (Heartland, WI) with a Canon Powershot S100 (Melville, NY) camera. Gel images were edited using Adobe Photoshop in a standardized manner: all gels were converted to grayscale and the auto-levels feature was used, without any additional manipulation, as needed.

## 2.5 Construction of Plasmids

Plasmids were constructed through PCR amplification of the desired insert, vector preparation (including PCR purification, restriction enzyme digestion, and gel extraction), In-Fusion® reaction and final confirmation of the construct through Sanger sequencing. In-Fusion® reactions were generally performed as follows: ~60 ng of restriction enzyme digested vector, no less than 20 ng of insert DNA, and 2 µl of 5X In-Fusion® HD Enzyme Premix were brought to a final reaction volume of 10 µl with HPLC-grade water. The reaction mixture was incubated in a 50°C water-bath for 15 minutes and then placed on ice. The reaction was either stored at -20°C or used to transform competent cells. Vector control reactions were performed side-by-side, without the addition of the desired insert DNA.

## 2.6 Transformation of *E. coli*

In order to propagate newly constructed plasmids, Stellar™ competent *E. coli* cells (Clontech Laboratories Inc., Mountain View, CA) were transformed with the plasmids. One 50 µl aliquot of competent cells was thawed on ice before being pipetted into a sterile

15 ml conical tube containing 2.5 µl of the final In-Fusion® reaction mixture. The reaction mixture was incubated on ice for 30 minutes before being heat-shocked in a 42°C water-bath for 45 seconds and immediately placed on ice. After 2 minutes, 450 µl of SOC medium (Clontech Inc.; Mountainview, CA) was added to the reaction and it was then incubated for 1 hour at 37°C on an orbital shaker set to 200 rpm. After the hour long incubation, 5 µl and 100 µl of the transformation mixture were spread onto LB plates supplemented with 100 µg/ml ampicillin. The remaining volume of the transformation was aseptically transferred to a sterile 1.5 ml microcentrifuge tube and pelleted for 3.5 minutes at 4000 rpm. The supernatant was decanted and the pellet was re-suspended in the residual media by vortexing and the concentrate was also plated on the appropriate media. The vector control In-Fusion® reaction transformation was performed side-by-side and 100 µl of the transformation reaction was plated. All plates were incubated at 37°C for 24 hours.

### 2.7 *S. aureus* Competent Cell Preparation (Nickoloff, 1995)

To prepare electrocompetent *S. aureus* cells, the desired strain was first grown overnight in TSB at 37°C with 200 rpm shaking. In a sterile Klett flask, 100 ml of fresh TSB was inoculated with 1 ml of the desired strain overnight culture. The culture was shaken at 37°C with 200 rpm shaking for approximately 3 hours, until Klett=95 (OD<sub>600</sub>=0.5) was reached. The Klett flask was immediately transferred to ice for 15 minutes to suspend bacterial growth. The culture was split between two 50 ml conical tubes, kept on ice at all times, and both were pelleted at 4°C for 15 minutes at 4000 rpm.

The supernatant was decanted and each cell pellet was re-suspended and washed with 15 ml ice-cold, sterile Milli-Q (EMD Millipore; Darmstadt, Germany) water before being re-pelleted at 4°C for 15 minutes at 4000 rpm. The wash step was repeated 2 more times for a total of 3 wash steps. Each cell pellet was then washed with 30 ml ice-cold sterile 10% glycerol and allowed to sit at room temperature for 15 minutes. The cells were pelleted at 4°C for 5 minutes at 4000 rpm and the supernatant was decanted. Each pellet was re-suspended in 300 µl of 10% ice-cold glycerol. The re-suspended cells were aliquoted (60 µl) and stored at -80°C.

### 2.8 Transformation of *S. aureus*

*S. aureus* electrocompetent cells (all RN4220 derivatives) were transformed by electroporation. One 60 µl aliquot of the desired electrocompetent cells was thawed on ice and 6 µl (0.3-0.6 µg) plasmid DNA were added to the thawed cells and allowed to sit for 30 minutes on ice. Pipette tips and cuvettes were kept at -20°C prior to being used. The reaction mixture was transferred to a 0.1 cm Gene Pulser® cuvette and electroporated on the STA setting (2.50 kV for 1 pulse, 2.5 ms) of a MicroPulser™ electroporation apparatus. Immediately after the pulse, 0.7 ml of brain heart infusion broth (BHI) was added directly to the cuvette and the cells were transferred to a 2 ml microcentrifuge tube containing an additional 0.3 ml BHI. Cells recovered by shaking at 32°C and 200 rpm for 2 hours. Cells were plated on TSA plates supplemented with appropriate antibiotics and/or X-gal, as needed. Generally, 5 µl, 100 µl and the cell pellet concentrate (pelleted at 4000 rpm for 3 minutes, supernatant decanted, pellet re-

suspended in residual supernatant) were spread and incubated for 48 hours at 32°C.

## 2.9 Allelic Exchange

*S. aureus* strains carrying derivatives of the pMAD allelic exchange vector were selected by plating on TSA plates supplemented with erythromycin (5 µg/ml) and X-gal (200 µg/ml) and incubated overnight at a permissive growth temperature, 32°C. Blue candidate colonies were chosen. TSB (2 ml) supplemented with erythromycin (5 µg/ml) was inoculated with a single colony and shaken overnight in a 42°C water-bath, which is a non-permissive growth temperature for the pMAD plasmid. Selection for antibiotic resistance at this temperature yields cells in which there has been homologous recombination of the plasmid carrying the desired mutation into the gene of interest in the *S. aureus* chromosome, yielding a cointegrate. All experiments were performed in quadruplicate. Samples were subcultured into 2 ml fresh TSB supplemented with erythromycin (5 µg/ml) and shaken overnight in a 42°C water-bath. This step was repeated a third time. The cultures were then 10-fold serially diluted to 10<sup>-5</sup> and 100 µl were spread on TSA plates supplemented with erythromycin (5 µg/ml) and X-gal (200 µg/ml) and incubated overnight at 42°C. Blue cointegrate colonies were chosen. TSB (5 ml) was inoculated with one blue colony and shaken overnight at 200 rpm at 30°C, a permissive temperature that encourages plasmid resolution. This step was repeated before samples were subcultured into 2 ml fresh TSB and shaken overnight at 42°C. This step was repeated twice. The cultures were 10-fold serially diluted to 10<sup>-5</sup> and 100 µl was spread on TSA plates supplemented with X-gal (200 µg/ml). Plates were incubated for 48 hours at 30°C. White colonies were patched onto TSA plates supplemented with

erythromycin (5 µg/ml) and X-gal (200 µg/ml) and onto TSA plates supplemented with only X-gal (200 µg/ml), in that order. Plates were incubated overnight at 30°C. White erythromycin-sensitive candidate colonies/patches that resolved the cointegrate and the plasmid were picked and plated on TSA plates supplemented with X-gal (200 µg/ml). Plates were incubated for 24-48 hours at 30°C. Candidate colonies were screened via colony PCR to ensure that the desired insert had homologously recombined and resolved and that the isolated candidate colony was not carrying an empty vector. After PCR screening, PCR clean-ups were performed using the QIAquick PCR Purification Kit (Qiagen; Valencia, CA), and allelic exchange candidates were verified by Sanger sequencing through Eurofins MWG Operon.

#### 2.10 Phage Propagation: Inductions

Lysogenic staphylococcal strains were induced in order to generate bacteriophage 80α phage lysates. Inductions were performed either through UV irradiation or the use of mitomycin C (MC). Both methods take advantage of the SOS response pathway which occurs in direct response to cellular DNA damage. Ten milliliters of a 25:1 solution of CY + GL media were inoculated with 50-100 µl of fresh overnight culture of the desired lysogenic *S. aureus* strain. CY media is a preparation of 1% wt/vol casamino acids, 1% wt/vol yeast extract, 0.5% wt/vol glucose, 0.59% wt/vol NaCl (Novick, 1991). GL media is composed of 0.6 M β-glycerophosphate disodium salt pentahydrate. Cell density was measured using a Klett-Summerson colorimeter until the starting cell density was approximately 10% of the final desired cell density. Cultures were grown at 30°C with 200

rpm shaking and cell density was monitored for several hours until the appropriate cell density was reached. For induction by UV irradiation, the final cell density was approximately Klett=95 or OD600=0.6, while cultures for MC induction were grown to Klett=30 or OD600=0.3.

For MC induction, equal volumes of SA phage buffer (Novick, 1991) (1 mM MgSO<sub>4</sub>, 4 mM CaCl<sub>2</sub>, 2.5 M Tris-HCl pH 7.8, 100 mM NaCl, 0.1% gelatin) and CY + GL media were combined. One milliliter of the Klett=100 culture was added to 9 ml CY + GL/ SA phage buffer. Two microgram per milliliter of MC was added to the culture mixture and then grown at 30°C with reduced shaking, 100 rpm, for approximately 2 hours or until cell lysis. Lysates were filter sterilized using a 0.22 µm syringe filter and stored at 4°C.

For UV induction, cultures were grown to Klett=30. Cultures were aseptically transferred to 15 ml conical tubes and centrifuged for 10 minutes at 4000 rpm at 4°C. The supernatant was discarded and the pellet was re-suspended in 5 ml of SA phage buffer. A conical tube containing 5 ml CY + GL buffer was prepared and set aside. The re-suspended cell pellet was transferred to a sterile petri dish, avoiding bubble formation. In a Nuaire Biological Safety Cabinet - Class II, Type A/B, equipped with a Philips TUV 15W/G15 Longlife bulb, the petri dish was placed on a rocker, the lid removed, and exposed to UV light for 20 seconds. The distance from the plate rocker to the UV bulb was approximately 57.8 cm. The prepared 5 ml CY + GL media was added immediately to the petri dish. The petri dish contents were transferred to a new, sterile Klett flask and incubated at 30°C with reduced shaking, 100 rpm, for approximately 2 hours or until cell lysis. Lysates were filter sterilized using a 0.22 µm syringe filter (Millipore; Billerica, MA) and stored at 4°C.

### 2.11 Bacteriophage Titering Assay

All titering assays were performed in triplicate. Five milliliter cultures of *S. aureus* RN4220 were grown overnight at 37°C in TSB with 200 rpm orbital shaking. Lysate dilutions were prepared as follows for both the control strain (RN10616) and the strain to be tested: 10<sup>-2</sup>, 10<sup>-3</sup>, 10<sup>-4</sup>, 10<sup>-6</sup>, 10<sup>-7</sup>, and 10<sup>-8</sup> dilutions of phage lysate in SA phage buffer. One hundred-fold dilutions were made by diluting 10 µl of lysate into 990 µl SA phage buffer. Ten-fold dilutions were made by diluting 100 µl of lysate into 900 µl SA phage buffer.

Top agar aliquots were prepared by mixing 3 ml of top agar with 30 µl of 0.5 M CaCl<sub>2</sub> (final concentration of 5 mM) and incubating at 65°C immediately prior to use. Phage top agar is composed of 0.3% wt/vol casamino acids, 0.3% wt/vol yeast extract, 100 mM NaCl, 0.75% wt/vol agar, pH 7.8 (Novick, 1991). One hundred microliters of the phage lysate dilution was mixed with 100 µl of the RN4220 overnight culture and allowed to adsorb for 3 minutes at room temperature. After adsorption, the top agar mixture was added to the 200 µl phage:RN4220 mixture and immediately poured onto phage agar plates and allowed to solidify at room temperature. Phage agar plates are composed of 0.3% wt/vol casamino acids, 0.3% wt/vol yeast extract, 100 mM NaCl, 1.5% wt/vol agar, pH 7.8 with 5 mM CaCl<sub>2</sub> added after media was autoclaved (Novick, 1991). Phage agar plates were incubated at 32°C for 24 hours before plaques were counted. Plaque forming units were calculated using the following equation:

$$\frac{\text{PFU}}{\text{ml}} = \frac{\text{number of plaques}}{(\text{d} \times \text{v})}$$

Where,  $d$  = dilution of plate counted

$v$  = volume of lysate dilution plated

### 2.12 SaPI1 Transductant Titering Assay

The quantification of SaPI1 transductants was accomplished through a modified phage-titer protocol, as described above. All SaPI derivatives used in this study contain a *tetM* cassette. As a result, SaPI1 strains were selected by plating on GL plates supplemented with 5  $\mu\text{g/ml}$  tetracycline. Serial dilutions were made following the phage-titer assay protocol: 100  $\mu\text{l}$  of lysate dilution was mixed with 100  $\mu\text{l}$  of RN4220 culture and allowed to adsorb at room temperature for 5 minutes. The 200  $\mu\text{l}$  lysate dilution:RN4220 mixture was poured onto GL-tet plates and allowed to solidify at room temperature before being incubated for 24-48 hours at 32° C. SaPI1 colonies or transducing units (TU) were calculated using the following equation:

$$\frac{\text{TU}}{\text{ml}} = \frac{\text{number of plaques}}{(d \times v)}$$

Where,  $d$  = dilution of plate counted

$v$  = volume of lysate dilution plated

### 2.13 Plaque Purification Assay

In order to isolate plaques for further analysis, individual plaques were cored from

the titer plates using a flame sterilized Pasteur pipette and expelled into a 1.5 ml microcentrifuge tube containing 1 ml of SA phage buffer. The agar core was allowed to stand at room temperature for 15 minutes before being serially diluted as follows:  $10^0$ ,  $10^{-1}$ ,  $10^{-2}$ ,  $10^{-3}$  and  $10^{-4}$ . Dilutions were prepared and plated, following the standard phage titering assay: 3 ml of top agar, supplemented with 30  $\mu$ l of 0.5 M  $\text{CaCl}_2$ , were prepared and kept at 65°C prior to use. One-hundred microliters of an overnight culture of RN4220 were mixed with 100  $\mu$ l of each lysate dilution and the phage were allowed to adsorb for 3 minutes at room temperature. The supplemented top agar was added to the phage dilution-cell mixture and immediately plated on phage agar. Plates were allowed to solidify at room temperature before being incubated for 24 hours at 32°C. Purified plaques were then cored and expelled into 1 ml HPLC-grade water. One microliter was used as the template to perform PCR amplifications of the mutant strain in order to confirm the mutation through Sanger sequencing.

#### 2.14 Data Analysis

All titer assay data were analyzed in GraphPad Prism® (La Jolla, CA). Raw data were organized in Microsoft® Excel® 2013 (Redmond, WA) and phage titers were calculated in PFU/ml. The phage titers were then imported into GraphPad Prism® and graphed. Phage titer assays were performed in biological and technical triplicate and all significant results were averaged and standard deviation was calculated.

## Chapter 3

### Investigation of the interface between 80 $\alpha$ scaffold and major capsid proteins

#### Introduction

Bacteriophage virion assembly begins with the formation of a transient procapsid, which eventually expands to form a mature virion. Procapsid assembly is important because without a properly formed procapsid, the subsequent capsid assembly steps will not occur, preventing the formation of viable phage progeny. The procapsid is an empty precursor particle that is comprised primarily of scaffold and capsid proteins. In addition, a portal protein and an uncharacterized minor capsid protein are involved in 80 $\alpha$  procapsid assembly. Scaffolding proteins act as a catalyst for procapsid formation by serving as molecular chaperones for the major capsid protein, leading to the nucleation of the major capsid proteins and eventual procapsid formation (Dokland, 1999). While this protein:protein interaction is critical to capsid assembly, little is known about the specific way in which 80 $\alpha$  scaffold and capsid interact. In the case of 80 $\alpha$ , the major capsid protein also interacts with the SaPI1-encoded alternative scaffolding protein, CpmB. These two capsid assembly pathways provide a unique model for the study of scaffold:capsid interaction.

The likely contacts between SaPI1 scaffold CpmB and 80 $\alpha$  capsid protein gp47 were mapped by a previous genetic study carried out in our lab. The two SaP1-encoded

capsid size redirection genes, *cpmA* and *cpmB*, were introduced into the capsid morphogenesis gene cluster of an 80 $\alpha$  prophage between gp44 (minor capsid protein) and gp46 (scaffold). This was lethal to lytic growth of the phage, because only small capsids that are unable to accommodate the larger phage genome were formed. This provided a strong selection for the loss of ability to form small capsids, as such mutants would restore phage growth. Rare viable phage plaques were isolated that restored the ability to form large capsids (E.A. Wall, unpublished). These mutants either carried deletions of *cpmA* and *cpmB* or point mutations in *cpmB*. Those in *cpmB* mapped to two regions, one being the dimer interface and the other being the very C-terminal end of the protein (Figure 3). While the SaPI1 scaffold and 80 $\alpha$  scaffold proteins are very different in size and share little overall amino acid similarity, there is a striking conservation of residues at their C-termini, particularly the RIKK motif where the *cpmB* mutations were found. This suggested that both scaffolds are interacting with the phage capsid protein in a similar way, likely involving the same region of capsid. Two questions were posed based on these results: (1) will these C-terminal scaffold mutations found in SaPI1 have the same effect if they are introduced into the 80 $\alpha$  scaffold protein? (2) Can we use these mutations in scaffold to isolate compensatory capsid mutations that would help identify where and how gp46 interacts with gp47?

#### Compensatory 80 $\alpha$ capsid mutations

The C-terminal point mutations that prevented small capsid formation in SaPI1 CpmB were R69S, R69K, and I70T (Figure 3; E.A. Wall, unpublished). Our strategy was to introduce similar mutations into the C-terminus of phage scaffold and then try to isolate

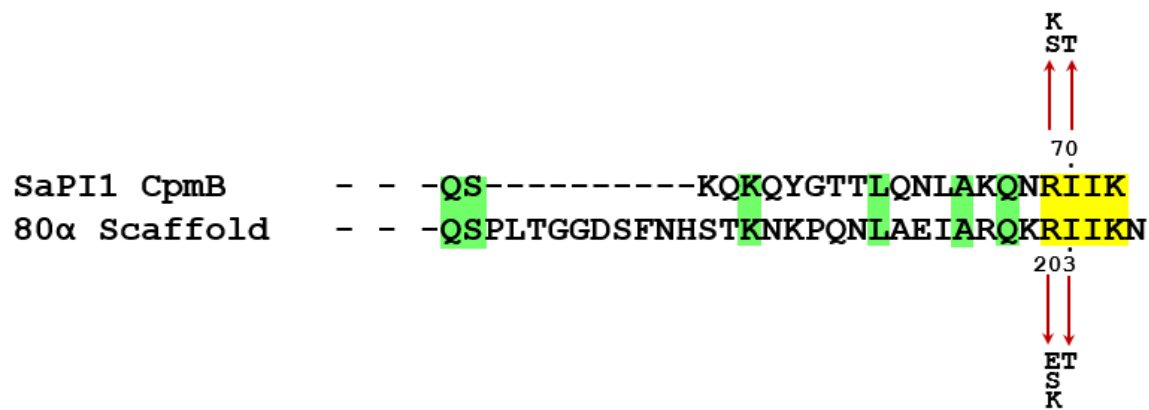


**Figure 3: Alignment of the C-termini of SaPI1 CpmB and 80α gp46**

Four C-terminal residues in the alternate SaPI1 scaffold protein, CpmB, and 80α scaffold protein, gp46, RIIK, are highly conserved. Not shown here are SaPI2 and SaPI3, which also contain conserved RIIK residues in their alternate scaffold proteins. The red arrows indicate rare compensatory mutations found in CpmB, following the expression of CpmA and CpmB in 80α, and the corresponding mutations subsequently introduced into the C-terminus of 80α scaffold.

spontaneous compensatory mutants in capsid. Because a single point mutation has a 1 in  $10^6$  likelihood of occurring spontaneously, all of our mutations were made using 2 nucleotide changes that would naturally occur at a rate of 1 in  $10^{12}$ . Since the standard 80 $\alpha$  lysate after prophage induction has a titer of approximately  $10^{10}$  PFU/ml, spontaneous revertants of the change in scaffold should be well below the limit of detection. The arginine to lysine mutation was not used in this study as there is no lysine codon that can be substituted that cannot revert to arginine by a single nucleotide change. Instead, the arginine was replaced independently with a glutamic acid and a serine. The serine and glutamic acid point mutations were introduced into an 80 $\alpha$  lysogen, resulting in R202S and R202E. It was predicted that the introduction of these point mutations into this highly conserved region of 80 $\alpha$  scaffold protein would force compensatory mutations in capsid that would re-establish the scaffold-capsid interface and therefore allow the production of viable phage. When these mutations were introduced, R202E and R202S were both lethal to the phage, as expected, underscoring the importance of the highly conserved C-terminal region of scaffold.

Unfortunately, neither point mutation at residue 202 in 80 $\alpha$  scaffold generated any spontaneous compensatory mutations. We next examined the effect of mutations introduced at residue 203, equivalent to CpmB residue 70. The same I to T mutation that inactivated CpmB was introduced into 80 $\alpha$  scaffold, resulting in a new 80 $\alpha$  lysogen carrying gp46 I203T. Upon UV induction and plaque titring, viable plaques were recovered at a low frequency (Figure 4). After plaque purification, several mutant candidates were sequenced to determine the nature of the mutations. Three distinct compensatory mutations were found in 80 $\alpha$  capsid: M52I, M52L, and Y123C.

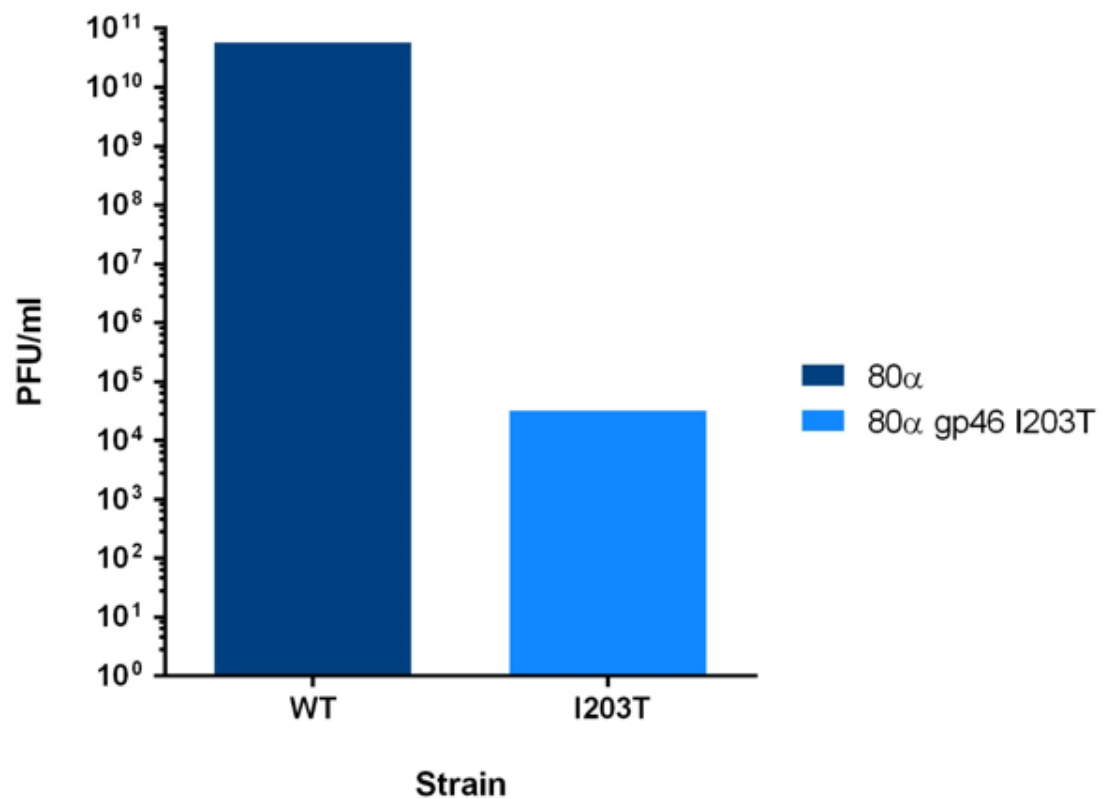


**Figure 4: Representative effect of gp46 I203T mutation on 80a phage titer.**

Wildtype 80α (RN10616) and 80α gp46 I203T (ST358) strains were grown to mid-exponential phase before being induced with 2 μg/ml of mitomycin C. The I203T scaffold mutants that formed plaques also contained compensatory capsid mutations.

## Effect of C-terminal scaffold mutations on SaPI1

Although SaPI1 CpmB acts as an alternate scaffold, the phage scaffold protein is still required. We predicted that another part of the larger phage scaffolding protein provided this “other” function, and that the presence of SaPI1 scaffold would substitute for the phage scaffold RIIK capsid interaction during formation of small procapsids. Therefore, we examined the effects of C-terminal 80 $\alpha$  scaffold mutations on SaPI1 transduction. Three separate 80 $\alpha$  lysogens containing mutations in the conserved C-terminal residues of scaffold, specifically R202E, R202S, and I203T, were transduced with SaPI1. When the original 80 $\alpha$  strains were induced and titered, as discussed above, all three resulted in a lethal phage phenotype. The strain encoding the I203T mutation in scaffold did result in the low level production of rare compensatory capsid mutations. The 80 $\alpha$  prophage in these SaPI1 transductions was induced, and both the phage and SaPI1 titers were determined. No SaPI1 transducing particles were recovered from either of the point mutations at residue 202. However, when the strain carrying the I203T mutant was induced and titered, SaPI1 transduction appeared to be normal. While these are preliminary results, they are notable as they indicate the SaPI1 scaffold does not simply replace the C-terminal contacts made by the phage scaffolding protein. The different behavior of the R202 mutants and the I203T mutant in supporting SaPI1 growth is not currently understood.

## Identifying the specific scaffold and capsid interface

Based upon a structural model of the SaPI1 scaffold CpmB mapped onto cryo-EM densities of the SaPI1 procapsid, (Dearborn et al., 2012), it appeared that an alpha-helix

of the C-terminal end of scaffold and an alpha-helix near the N-terminus of capsid formed a parallel interface. The compensatory mutations M52I and M52L map to a residue within a predicted alpha-helix near the N-terminus of capsid. This residue is flanked by two glutamic acids at residues 50-53 (EVME). This led to the hypothesis that the conserved and critical C-terminal R202 residue in scaffold could interact with and possibly form a salt-bridge with one of the glutamic acid residues in 80 $\alpha$  capsid (Figure 5). The protein stabilization created by the interaction of the guanidinium group of arginine and the side chain carboxyl of glutamic acid would contribute to maintenance of the proper alpha-helical interaction between scaffold and capsid (Figure 6). Recently, Cortines et al. have shown that a specific salt-bridge interaction between the C-terminal scaffold residue R293 and the N-terminal capsid residue D14 in bacteriophage P22 is enough to establish the proper protein:protein interaction for successful procapsid assembly.

To test the hypothesis that R202 interacts with E50 or E53, four new strains containing 80 $\alpha$  prophages with scaffold and capsid mutations were constructed: gp47 E50R (ST375), gp47 E53R (ST376), gp46 R202E + gp47 E50R (ST377), and gp46 R202E + gp47 E53R (ST378). The prediction was that at least one of the capsid mutations, E50R or E53R, would be lethal, due to the inability to form a salt bridge with R202. The R202E scaffold mutation, on its own, is lethal. However, if the salt-bridge interaction was occurring at the proposed residues, then it was anticipated that the simultaneous replacement of R with E in scaffold and E with R in capsid would lead to the re-establishment of the salt-bridge interaction and rescue the lethal R202E scaffold phenotype, resulting in viable progeny phage. All four strains were induced using MC, and plaque titer assays were performed. Surprisingly, both single capsid mutant strains,

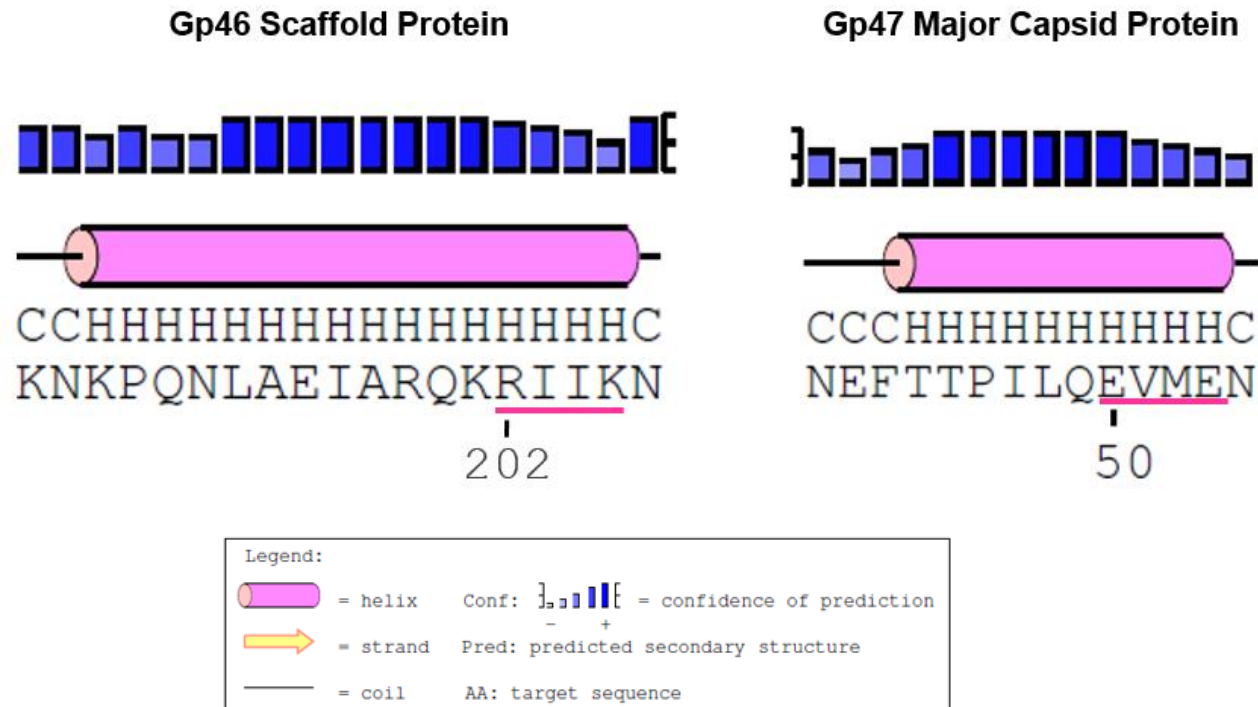


**Figure 5: Predicted secondary structure of the hypothesized alpha-helical interaction site between gp46 (scaffold protein) and gp47 (major capsid protein).**

The predicted secondary structures of gp46, scaffold protein, and gp47, major capsid protein. The PSIPRED v3.3 Protein Sequence Analysis Workbench was used to generate predicted secondary structure.

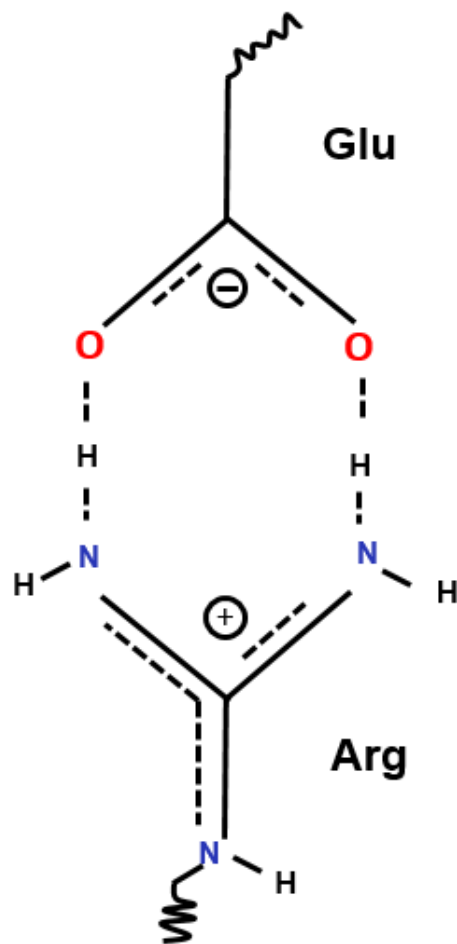


**Figure 6: Schematic of the proposed salt-bridge interaction between R202 in gp46 and either E50 or E53 in gp47.**

The non-covalent protein-protein interactions established by the salt-bridge between R202 and E50 or E53 may be enough to establish the proper helical interface for successful procapsid assembly.

ST375 and ST376, behaved like wild-type 80 $\alpha$ , indicating that neither glutamic acid in capsid was essential or specifically interacting in a critical way with the arginine in scaffold (Figure 7). Similarly, both of the double phage mutants remained non-viable (Figure 8). This indicates that the predicted salt bridge contact between R202 in phage scaffold, and either E50 or E53 in phage capsid, was incorrect.

## Discussion

Mutations in the C-terminal end of scaffold gave rise to compensatory mutations, M52I and M52L, within the predicted alpha-helix in phage capsid, indicating that this region of capsid does make contact with the scaffold C-terminus. However, the predicted salt bridge interaction involving one of the flanking glutamic acid residues was not ruled out by this study. The lethality of the R to K substitution in scaffold still argues strongly for a salt bridge interaction. Recent studies have indicated that single amino acid salt-bridge interactions are able to sustain proper protein:protein interaction for successful procapsid assembly in a similar way to our current model. The C-terminal domain of the P22 scaffolding protein is alpha-helical, which is comparable to the predicted C-terminal alpha-helix of the 80 $\alpha$  scaffold protein. Again, similar to our model, the N-terminal alpha-helix of the major capsid protein of P22 is thought to interact with the N-terminal region of scaffold (Cortines et al. 2014). However, Cortines et al. also indicated other nearby amino acids that played a stabilizing role in the salt-bridge interaction between the major capsid protein and scaffold protein of P22, but were not essential. It seems likely, therefore, that

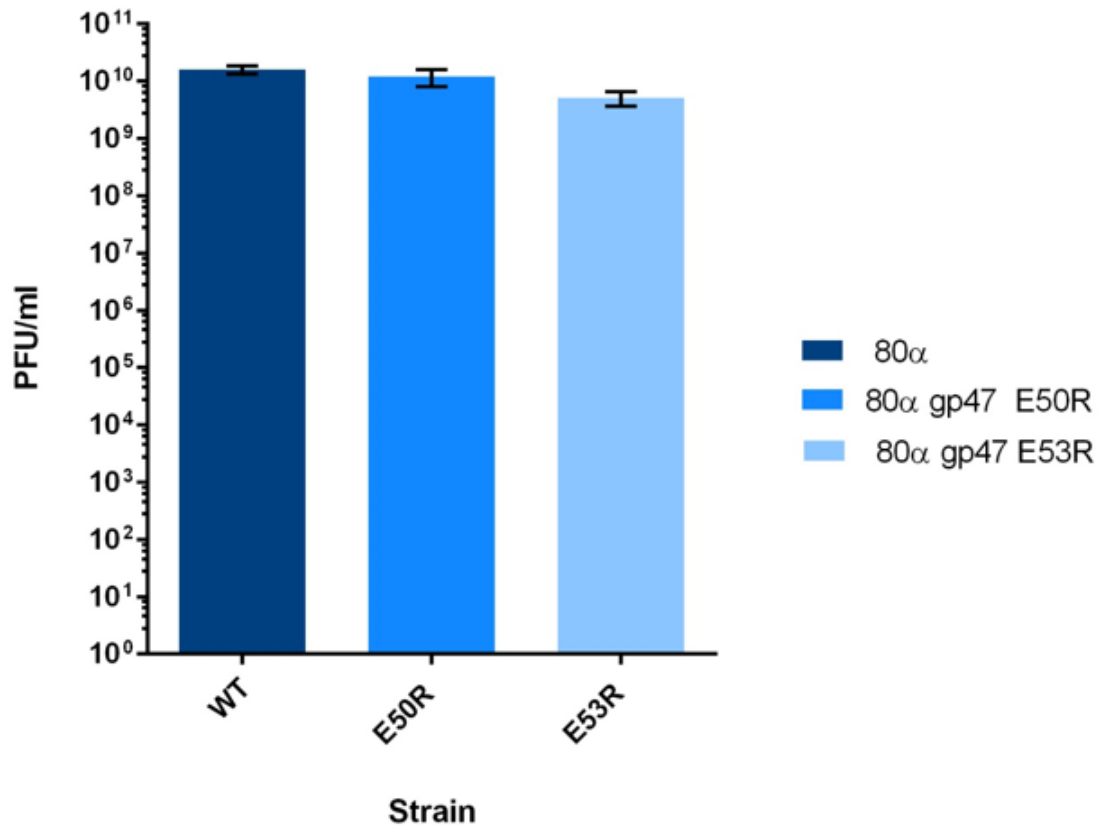


**Figure 7: Effect of E50R and E53R gp47 major capsid protein mutations on 80α phage titer.**

Strains lysogenic for wild type 80α (RN10616), 80α gp47 E50R (ST375) and 80α gp47 E53R (ST376) were grown to mid-exponential phase before being induced with 2 μg/ml of mitomycin C. Each bar is the result of 3 independent experiments, and the error bars indicate standard deviation.

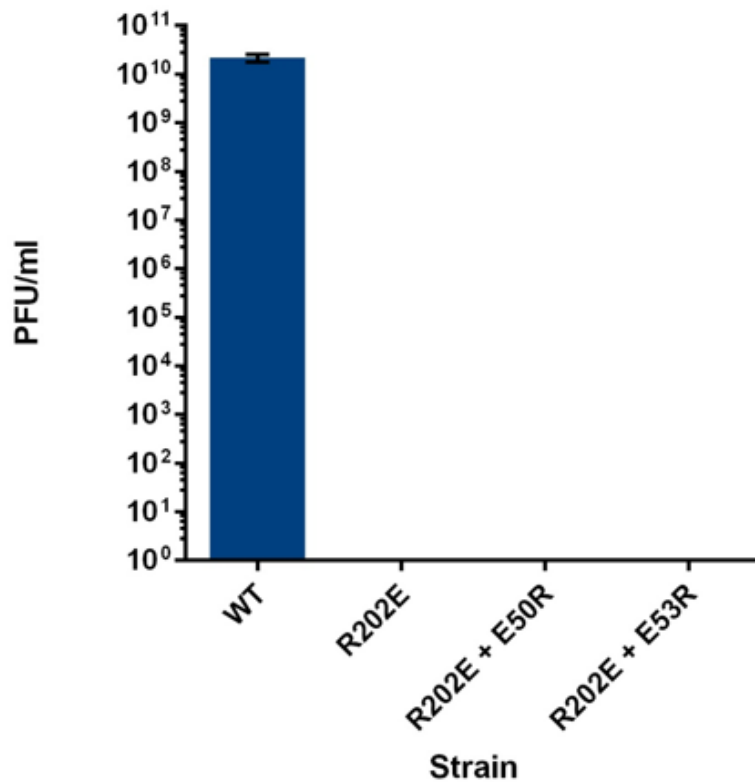


**Figure 8: Effect of E50R and E53R gp47 major capsid protein mutations paired with an R202E gp46 scaffold mutation on 80 $\alpha$  phage titer.**

Strains lysogenic for wild-type 80 $\alpha$  (RN10616), 80 $\alpha$  R202E (ST279), 80 $\alpha$  gp46 R202E + gp47 E50R (ST377), and 80 $\alpha$  gp46 R202E + gp47 E53R (ST378) were grown to mid-exponential phase before being induced with 2  $\mu$ g/ml of mitomycin C. Each bar is the result of 3 independent experiments, and the error bars indicate standard deviation.

there is a salt bridge interaction involving a different E or D residue located near this helix in the 3-D structure of capsid that remains to be identified.

Of note is the third compensatory capsid mutation that was isolated from the scaffold I203T mutant strain: Y123C. In 80 $\alpha$  capsid, there is an integral proline at residue 132 in the procapsid. This proline forms a kink in the  $\alpha$ -helix and allows the structural rearrangement that accompanies a conformational switch necessary for expansion of the procapsid to the mature capsid (Spilman et al., 2011). Based on an I-TASSER model of 80 $\alpha$  capsid mapped onto the HK97 fold, Y123 is predicted to be on the same alpha-helix as P132. At this time, the biological implications of this compensatory mutation have not been fully examined.

## Chapter 4

### **The role of N-terminal cleavage of scaffold and major capsid proteins in staphylococcal phage 80 $\alpha$ and SaPI1**

#### Introduction

Unlike other bacteriophages characterized to date, 80 $\alpha$  does not encode a prohead protease, but rather uses a host-encoded protease for N-terminal cleavage of both its scaffold (gp46) and major capsid (gp47) proteins (Spilman et al., 2012). When the genes encoding gp46 and gp47 were cloned into an *E. coli* expression vector and expressed, neither protein was cleaved. However, when gp46 and gp47 were coexpressed in *S. aureus*, both proteins underwent proteolytic processing to a cleaved form (Spilman et al., 2012), identical to those found in mature virions (Poliakov et al., 2008). The host-encoded protease responsible for the N-terminal cleavage of scaffold and capsid was recently identified as the phage-related ribosomal cysteine protease, Prp (Wall et al., 2015). Prp removes the first 13 amino acids from gp46 and the first 14 from gp47 by cleaving between phenylalanine and alanine in a conserved motif. Capsid cleavage apparently occurs even in the absence of capsid assembly. Therefore, we wanted to investigate the requirements for scaffold and capsid cleavage in the assembly of both phage and SaPI capsids.

### N-terminal cleavage of scaffold

A mutant allele of the scaffold gene expressing the cleaved version of the protein (accomplished by deletion of amino acids 2-13) was introduced into an 80 $\alpha$  prophage through allelic exchange to generate strain ST247. The “precleaved” 80 $\alpha$  (gp46 $\Delta$ 2-13) lysogen was induced by UV irradiation and titered following the standard plaque assay. No viable phage were recovered (Figure 9).

Previous studies have demonstrated that scaffold is essential for formation of 80 $\alpha$  capsids. Strain ST91, an 80 $\alpha$  lysogen in which *orf46* has been deleted, was induced, and the resulting lysate was purified and examined via electron microscopy (EM) (Spilman et al., 2012). Experiments replicating this result and comparing it to the structures assembled after induction of the pre-cleaved scaffold mutant in ST247 were performed by Keith Manning in Dr. Terje Dokland’s lab (Figure 10). As can be seen in Figure 10, both the complete deletion of gp46 and the pre-cleaved form of gp46 result in strikingly similar phenotypes. While the characteristic non-contractile tails and baseplates of 80 $\alpha$  were observed, no procapsids or mature capsids were seen. This indicates that the cleavage of gp46 is essential and that improper regulation or timing of cleavage is as detrimental to 80 $\alpha$  as the complete absence of scaffold.

### Effect of scaffold mutations on SaPI1

80 $\alpha$  capsid is unique in its ability to interact with not only its own native phage scaffold, but also the alternate scaffold formed by SaPI1. However, the SaPI1-encoded alternate scaffold is unable to substitute completely for phage scaffold (Spilman et al., 2012). Therefore, we wanted to examine the role of scaffold cleavage in formation of

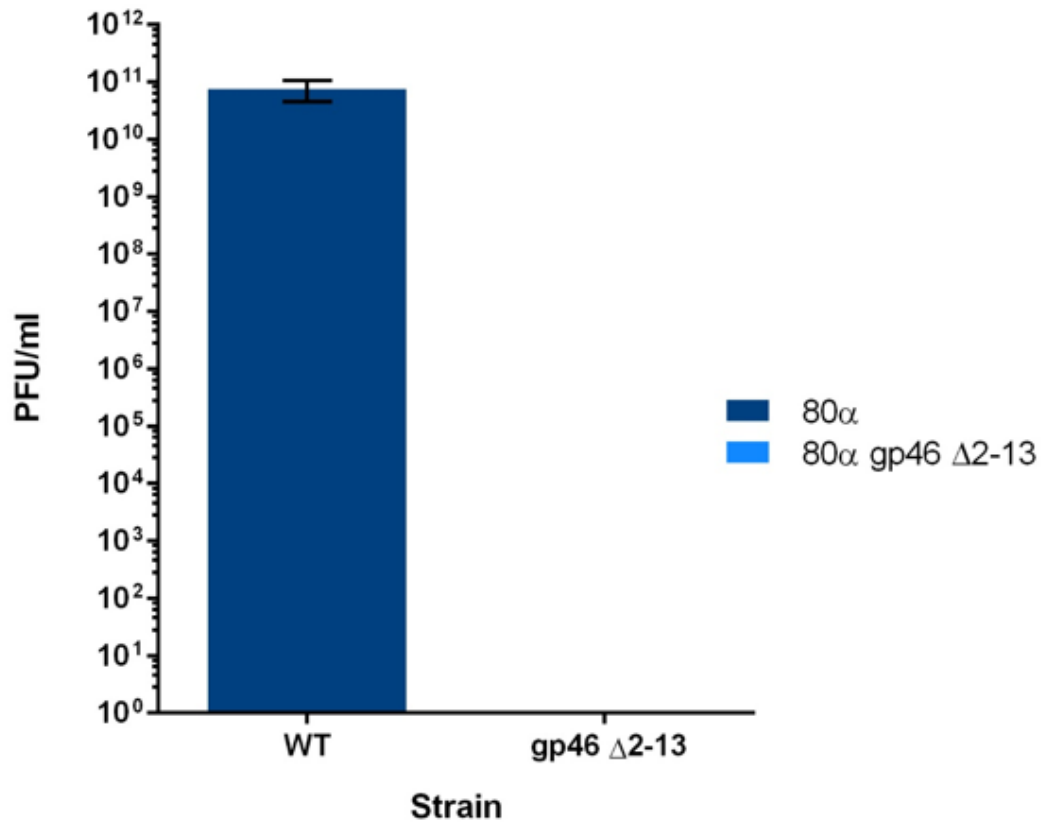


**Figure 9: Effect of N-terminally cleaved scaffold on 80α titer.**

Strains carrying prophage of wild-type 80α (RN10616) and 80α with N-terminally cleaved gp46 Δ2-13 (ST247) were grown to mid-exponential phase before being induced with 2 μg/ml of mitomycin C, and the resulting lysates were titered on RN4220. Each bar is the result of 3 independent experiments, and the error bars indicate standard deviation.

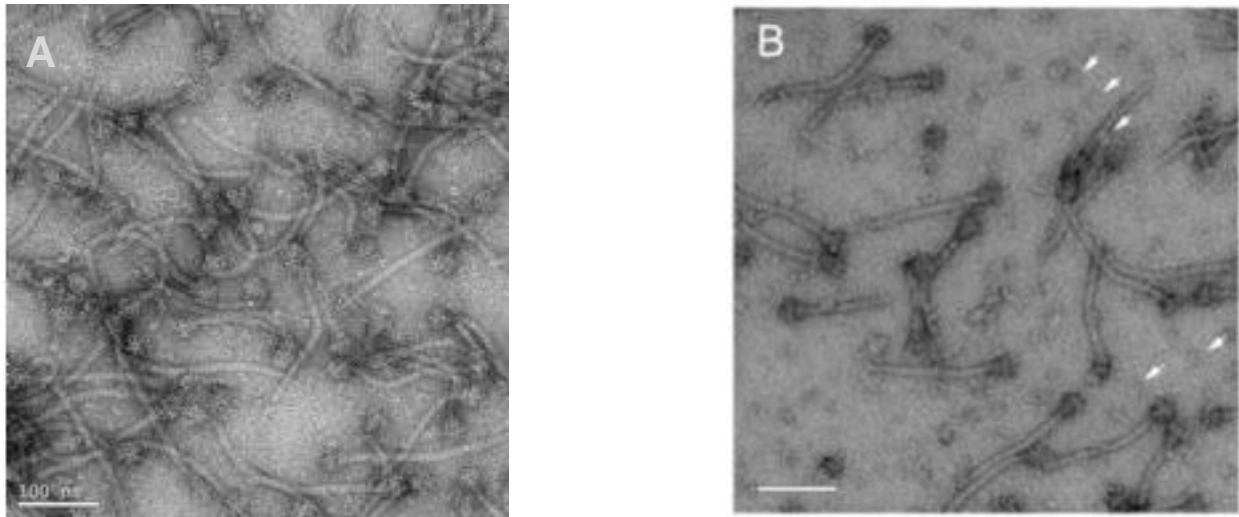


**Figure 10: Electron micrographs of CsCl purified 80 $\alpha$  phage structures from scaffold mutants.**

EMs used with permission of Dr. Terje Dokland. Scale bar indicates 100 nm. Phage suspensions for negative stain were applied to glow-discharged carbon-only grids (Electron Microscopy Sciences), washed twice with dialysis buffer and stained with 1% uranyl acetate. Samples were observed in an FEI Tecnai F20 electron microscope operated at 200kV. Images were captured on a 4k x 4k Gatan Ultrascan CCD camera.

(A) EM of structures formed by induction of an 80 $\alpha$  lysogen encoding pre-cleaved scaffold (ST247).

(B) EM of structures formed induction of an 80 $\alpha$  lysogen encoding scaffold deletion (ST91). White arrows indicate possible portal structures, not procapsids.

SaPI1 transducing particles. SaPI *tst:tetM* was introduced by transduction into the strain carrying the 80 $\alpha$  (gp46 $\Delta$ 2-13) prophage to yield strain ST365. The resulting lysate was titered for SaPI1 transducing particles following UV induction. While this experiment has only been carried out once thus far and must be considered preliminary, SaPI1 was able to transduce effectively.

Additionally, we wanted to examine the effects of C-terminal 80 $\alpha$  scaffold mutations on SaPI1 transduction. In particular, we wanted to test whether the wild-type SaPI1 alternate scaffold could substitute for phage scaffold that was defective in the similar C-terminal contacts with capsid. SaPI1 was transduced into an 80 $\alpha$  lysogen containing mutations in the conserved C-terminal residues of scaffold, specifically R202E, R202S, and I203T, resulting in the following strains: ST366 (80 $\alpha$  gp46 R202S), ST367 (80 $\alpha$  gp46 R202E), and ST368 (80 $\alpha$  gp46 I203T). As described in Chapter 3, all three of these mutations prevented 80 $\alpha$  plaque formation, and the I203T mutation gave rise to rare compensatory capsid mutants. When the strains carrying mutant R202E and R202S prophages plus SaPI1, were induced and titered, no SaPI1 transducing particles were recovered. However, when the strain encoding the I203T mutant was induced and titered, SaPI1 transduction appeared to occur at wild-type levels. These results are notable as they indicate SaPI1 does not require the N-terminal cleavage of 80 $\alpha$  scaffold to transduce effectively. However, C-terminal point mutations in 80 $\alpha$  scaffold, specifically R202E and R202S, block SaPI1 transduction, demonstrating that SaPI1 does not simply replace the contacts between the scaffold C-terminus and the capsid N-terminus with its own scaffold-capsid interaction. The difference between the results obtained with the R202 mutants and the I203T mutant remains to be explained.

### Effect of uncleavable capsid on 80 $\alpha$ growth

The role of capsid cleavage in 80 $\alpha$  was investigated by introducing the mutation F14A into the cleavage motif. This prevents cleavage of the capsid protein. This mutant allele was introduced into an 80 $\alpha$  prophage and assayed for plaque formation following UV induction. Surprisingly, this mutation resulted in viable phage with a titer that was not significantly different from wild-type titer (Figure 11). While N-terminal cleavage of scaffold is essential for the production of viable phage virions, cleavage of the capsid protein is not essential for proper capsid formation.

The result with uncleavable capsid has been confirmed in a slightly different background, RN450. Our uncleavable capsid strain, ST361, was constructed in the strain RN4220. RN4220 is a restriction-minus derivative strain of RN450 (Novick, 1967; Kreiswirth et al. 1983). Strain ST208, which also contains a prophage with uncleavable capsid (gp47 F14A) is in the RN450 background. Figure 12 presents unpublished data from our collaborator's lab of cryo-EM images obtained after the induction and purification of ST208 lysates. Both wild-type 80 $\alpha$  and uncleavable capsid are strikingly similar in their mature capsid formation, providing further evidence that the cleavage of major capsid protein is not required for phage viability. Furthermore, 3-D reconstruction of the cryo-EM images display extra density on the outside of the capsids, attributable to the extended N-terminal residues (data not shown).

### Discussion

These data indicate that the cleavage of gp46 during assembly is an essential process in the formation of phage capsids. It is hypothesized that the N-terminal tail of

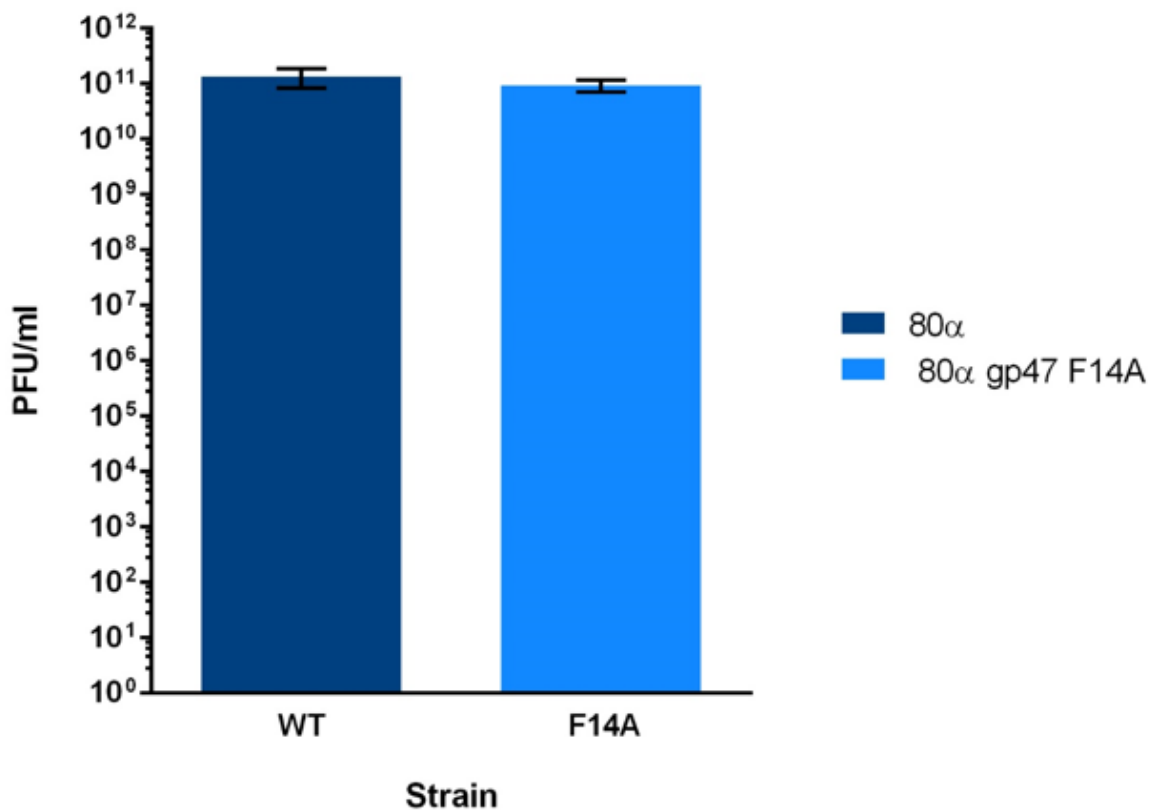
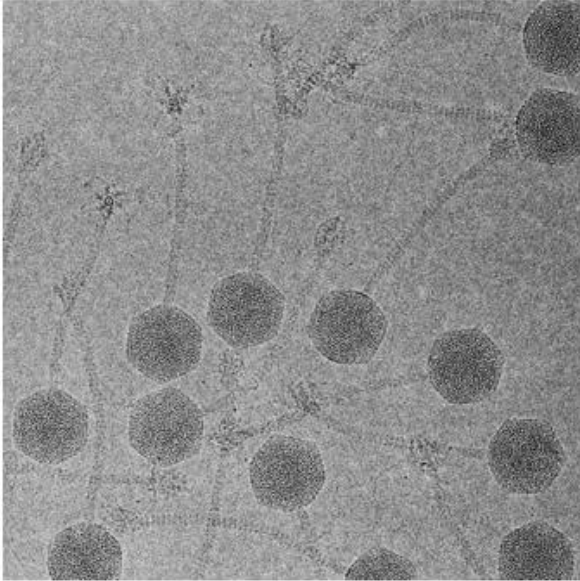


**Figure 11: Effect of uncleavable capsid protein, gp47, on 80α phage titer.**

Strain carrying lysogens of wild-type 80α (RN10616) and 80α gp47 F14A (ST361), uncleavable capsid protein, strains were grown to mid-exponential phase before being induced with 2 μg/ml of mitomycin C and titered on RN4220. Each bar is the result of 3 independent experiments, and the error bars indicate standard deviation.

**A**



**B**

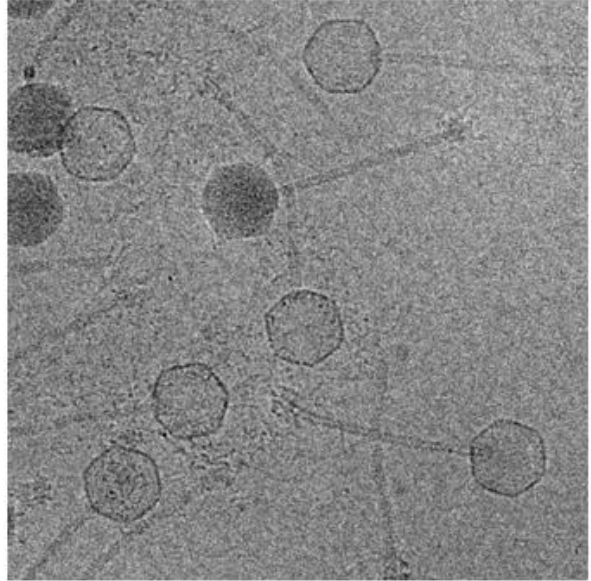


**Figure 12: Cryo-EM of capsid formation in wild-type 80 $\alpha$  (A) and uncleavable capsid (gp47 F14A) (B).**

EMs used with permission of Dr. Terje Dokland. Samples of purified phage lysate were applied to C-flat holey film (Electron Microscopy Sciences), flash frozen, transferred to a Gatan 626 cryo-specimen holder and visualized in an FEI Tecnai F20 electron microscope operated at 200 kV at a magnification of 81,200x.

scaffold may play a role in stabilization during procapsid formation, as scaffold serves as a chaperone for the proper accumulation of capsid, and therefore proper procapsid assembly. Without this interaction, no viable phage progeny are produced. However, this cleavage event is apparently not required for efficient SaPI1 transduction. SaPI1 transduction by the 80 $\alpha$  gp46 $\Delta$ 2-13 prophage in ST247 remarkably resulted in viable transducing particles even though ST247 alone cannot produce viable phage. This suggests that a SaPI1 gene product, possibly the alternate scaffold, CpmB, can substitute for this particular function of phage scaffold. The respective roles of SaPI1 and phage scaffold proteins in assembly of SaPI transducing particles are still not well understood. Previous experiments determined that deletion of 80 $\alpha$  gp46 resulted in both dead phage and no SaPI1 transducing particles, so SaPI1 is clearly dependent on phage scaffold in some way (Spilman et al., 2012).

One hypothesis for the presence of viable SaPI1 transducing particles is that a virion structure is formed in the pre-cleaved scaffold mutant but it is unable to produce viable phage, possibly because it is unable to expand to mature capsid. In that case, the genome of 80 $\alpha$  would not be packaged, but the smaller SaPI1 genome could still be accommodated. However, the EMs of ST247 do not reveal any procapsid formation, indicating that SaPI1 must be compensating in some way to allow capsid assembly, possibly via the alternative scaffold, CpmB. Additionally, if the N-terminus of phage scaffold is required for Prp binding and chaperone function, maybe SaPI1 CpmA can function as an alternative chaperone for assembly of the smaller SaPI1 procapsids. Another possibility would be that full length gp46 is needed for the proper localization of gp44, the minor capsid protein, in the procapsid in addition to its role as a chaperone

protein for capsid. Prior work in our lab has demonstrated that gp44 is essential for the phage, but not for SaPI1.

While cleavage of gp46 is essential, N-terminal cleavage of gp47 is most notably not. Strain ST361 induction and plaque titering revealed that uncleavable gp47 behaves similarly to wild-type 80 $\alpha$ . This suggests that the extra N-terminal 13 amino acids can be accommodated in the mature capsid without affecting capsid integrity. This result was surprising, and raises the question of why the phage has retained the cleavage motif. One possibility is that Prp functions as a chaperone for assembly in addition to its role as a protease, and this sequence is required for Prp binding.

## Chapter 5

### Discussion

The purpose of this work was to characterize the interactions between staphylococcal phage 80 $\alpha$  scaffold and capsid proteins and their roles in functional capsid assembly. Capsid assembly is a multi-step, complex process that is predicated by the proper assembly of a transient procapsid structure. Like all tailed bacteriophages, multiple copies of the internal scaffolding protein of 80 $\alpha$  and the HK97-like major capsid proteins nucleate and self-assemble into a procapsid structure (Suhanovsky et al., 2015). Following a dramatic conformational change involving the dynamic “switch” of P132 in capsid, the procapsid expands, internal scaffold proteins are lost, DNA is packaged, and external capsid proteins rearrange, finally forming a mature icosahedral capsid that contains the entire 80 $\alpha$  genome (Spilman et al., 2011). Unlike other tailed phages, the 80 $\alpha$  capsid assembly process can be hijacked by a mobile genetic element, SaPI1. SaPI1 is able to redirect capsid assembly via two SaPI1 encoded genes, *cpmA* and *cpmB*, and instead of forming large capsids, preferentially forms smaller transducing particles that package SaPI DNA, in lieu of the 80 $\alpha$  genome. Of particular note is the presence of an alternate SaPI1 scaffold protein, CpmB. It is this unique instance, where two distinct scaffold proteins interact with the same capsid protein in strikingly similar ways, which allowed us to explore not only location of the protein:protein interface between scaffold

and capsid, but also the roles of scaffold and capsid cleavage in the context of 80 $\alpha$  and SaPI1.

#### Investigating 80 $\alpha$ scaffold and capsid protein interactions

It was predicted by our lab that the 80 $\alpha$  scaffold and capsid proteins formed a stable interface through the formation of a non-covalent salt bridge between a C-terminal R202 residue in scaffold and a glutamic acid in capsid (either residue E50 or E53). This prediction arose from a structural model, based upon the cryo-EM densities of SaPI1 scaffold, CpmB, mapped onto a SaPI1 procapsid, but also from genetic evidence from previous work in our lab. This interaction was tested in various ways. First, the predicted alpha-helix in capsid, containing the EVME motif of interest (residues 50-53), was mutated separately at two sites, resulting in two single capsid mutant strains carrying an 80 $\alpha$  prophage with either an E50R or E53R capsid mutation. If our hypothesis had been correct, and the arginine-glutamic acid interaction was disrupted by either of these mutations, the 80 $\alpha$  titer would likely have been reduced, if not completely abolished. However, both strains behaved similarly to wild-type 80 $\alpha$ . The next step was introducing these same capsid mutations into a known lethal phage background, specifically gp46 R202E. In these strains, the hypothesized salt bridge interaction was reversed, with the glutamic acid of capsid now residing in scaffold, and vice versa. Both double mutant strains were still non-viable, indicating that the lethal R202E phenotype was unable to be rescued by a putative re-established salt bridge.

While this region of capsid does appear to directly interact with the C-terminal end of scaffold, based on the I203T second site suppressor mutants M52I and M52L, it fails

to establish the predicted salt-bridge interaction. However, there is a very similar motif nearby at residues 64-67, EPME. These motifs are not identical, however valine and proline are both non-polar and hydrophobic. While this similar motif is interesting, there are several issues that need to be resolved. First, when the I203T scaffold mutation was introduced into 80 $\alpha$ , compensatory capsid mutations were found in the predicted helical region of capsid, at residue 52. Additionally, the EVME motif resides in an alpha-helix, whereas EPME appears to be in a beta strand, according to the predicted secondary structure created in PSIPRED. This poses a problem as the conserved residues of scaffold, RIIK, are also located in an alpha-helix. The long held assumption has been that scaffold and capsid are interacting via their respective C-terminal and N-terminal alpha-helices. An I-TASSER model was constructed where 80 $\alpha$  capsid was modeled onto the HK97-fold (Figure 10). This model appears to conflict with the PSIPRED predicted alpha-helical regions of C-terminal scaffold and N-terminal capsid, as they both appear to be found on beta sheets. However, the I-TASSER model score of -0.6 suggest this model is not robust. Both the PSIPRED prediction, and the I-TASSER model underscore the need for an improved structural model of 80 $\alpha$  scaffold:capsid interaction. Additionally, the N-terminus of phage scaffold has not been completely modeled, as a result, the EVME region could lie close to another region that establishes the salt bridge, however, with the current model this cannot be determined.

#### Future directions for identifying the interface between scaffold and capsid proteins

While molecular models can be helpful, currently all of these structures are based on predictions. Previously, our lab has used the bacterial adenylate cyclase two-hybrid

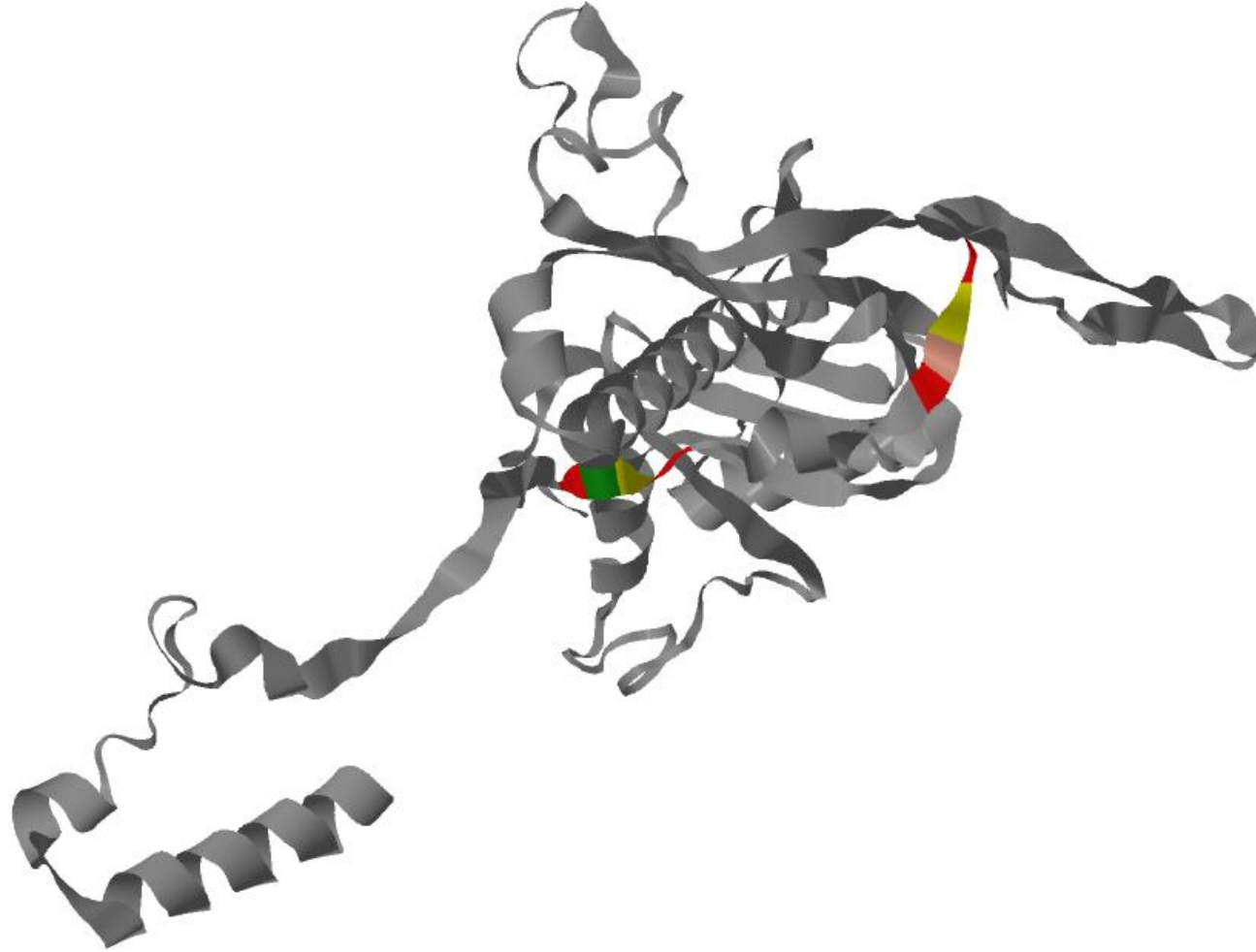


**Figure 13: I-TASSER model of gp46 modeled onto the HK97-fold.**

Red indicates glutamic acid residues, yellow indicates methionine, green indicates valine, and pink indicates proline. The following residues are indicated on the model: EVME (residues 50-53) and EPME (residues 64-67). Geneious 6.1 Bioinformatics software was also used in generating this image.

system (BACTH) (Euromedex; Souffelweyersheim, France) to investigate the protein:protein interactions between scaffold and capsid. The BACTH system provides a much quicker screening tool than our current experimental approach which involves the very time intensive process of performing allelic exchanges, induction experiments and plaque titering assays.

The BACTH system is based upon the reconstitution of adenylate cyclase activity through the interaction of two proteins fused to its fragmented catalytic domain (Karimova et al., 2000; Battesti et al., 2012). The catalytic domain of adenylate cyclase has two subdomains that are known to interact with each other, referenced here as T18 and T25. In the BACTH system used in our lab these two subdomains are inactive when they are separated. As such, the two subdomains can be fused to two different polypeptides in order to ascertain whether or not the polypeptides interact with each other. Upon transformation and coexpression of the two fusion proteins in an *E. coli* reporter strain lacking chromosomal adenylate cyclase, the two subdomains can heterodimerize due to an interaction between the polypeptides being tested, reconstituting the catalytic domain and resulting in active synthesis of cAMP. The newly synthesized cAMP can go on to bind the catabolite activator protein, CAP, which then binds to the promoter of the lactose or maltose operon, inducing gene expression (Battesti et al., 2012). Through this system, after creating the desired constructs, protein:protein interactions can be visualized through blue/white screening ( $\beta$ -galactosidase expression is regulated by cAMP/CAP) or plating on another appropriate indicator media, such as MacConkey agar, which indicates whether or not maltose is metabolized.

When the first 90 N-terminal residues of 80 $\alpha$  capsid were fused to the T18 fragment and the last 70 C-terminal residues of 80 $\alpha$  scaffold protein were fused to the T25 fragment, the blue/white screening results were inconclusive. It is possible that these terminal fragments, particularly the N-terminus of capsid, do not assume the proper conformation. The next step in this process would be to screen the full-length proteins using the BACTH system, rather than the previously tested polypeptides. Besides the BACTH system, the more established yeast two-hybrid system could also be used to approach this problem.

#### N-terminal cleavage of 80 $\alpha$ scaffold and capsid proteins

Previous studies have demonstrated that only cleaved capsid is present in mature 80 $\alpha$  virions. Phage scaffold, found in procapsids trapped by a mutation in terminase that blocks DNA packaging, is also N-terminally cleaved. However, the timing of this cleavage event is not well defined. Pre-cleaved scaffold and uncleavable capsid both have striking phenotypes: pre-cleaved scaffold is completely lethal, akin to the complete deletion of scaffold, and uncleavable capsid behaves like wildtype 80 $\alpha$ . Future experiments are already in progress in which 80 $\alpha$  lysogens carrying pre-cleaved capsid and uncleavable scaffold mutations will be induced and titered in order to observe their effects on phage capsid assembly. In addition to plaque assays, EMs of the resulting lysates would also be helpful in detecting any structural discrepancies generated by these mutations. Once all four cleavage strains have been tested, it will be interesting to see if the N-terminus of

capsid is necessary for scaffold-mediated chaperoning, or if scaffold is interacting with a different area of capsid for this purpose.

In this work, we determined that similar residues at the C-termini of phage and SaPI1 scaffolds are required for proper procapsid assembly. However, the C-terminal residue of 80 $\alpha$  scaffold R202 and the early N-terminal E50 or E53 residues in capsid were not involved in a proposed salt bridge interaction. This implies that these two  $\alpha$ -helices are not solely responsible for forming the interface between scaffold and capsid necessary for capsid assembly, although the I203T compensatory mutants indicate that these two regions do interact. Additionally, we have also determined that the timing of scaffold cleavage is significant. Pre-cleaved scaffold results in an inability to form viable phage progeny, analogous to the complete deletion of scaffold. Uncleavable capsid behaves comparably to wild-type 80 $\alpha$ , indicating that N-terminal cleavage of capsid is not essential.

## References

Archer, G. (1998). *Staphylococcus aureus*: A Well–Armed Pathogen. *Clinical Infectious Diseases*, 26(5), pp.1179-1181.

Arnaud, M., Chastanet, A. and Debarbouille, M. (2004). New Vector for Efficient Allelic Replacement in Naturally Nontransformable, Low-GC-Content, Gram-Positive Bacteria. *Applied and Environmental Microbiology*, 70(11), pp.6887-6891.

Battesti, A. and Bouveret, E. (2012). The bacterial two-hybrid system based on adenylate cyclase reconstitution in *Escherichia coli*. *Methods*, 58(4), pp.325-334.

Christie, G. and Dokland, T. (2012). Pirates of the Caudovirales. *Virology*, 434(2), pp.210-221.

Christie, G., Matthews, A., King, D., Lane, K., Olivarez, N., Tallent, S., Gill, S. and Novick, R. (2010). The complete genomes of *Staphylococcus aureus* bacteriophages 80 and 80 $\alpha$ —Implications for the specificity of SaPI mobilization. *Virology*, 407(2), pp.381-390.

Cortines, J., Motwani, T., Vyas, A. and Teschke, C. (2014). Highly Specific Salt Bridges Govern Bacteriophage P22 Icosahedral Capsid Assembly: Identification of the Site in Coat Protein Responsible for Interaction with Scaffolding Protein. *Journal of Virology*, 88(10), pp.5287-5297.

Damle, P., Wall, E., Spilman, M., Dearborn, A., Ram, G., Novick, R., Dokland, T. and Christie, G. (2012). The roles of SaPI1 proteins gp7 (CpmA) and gp6 (CpmB) in capsid size determination and helper phage interference. *Virology*, 432(2), pp.277-282.

Dearborn, A., Spilman, M., Damle, P., Chang, J., Monroe, E., Saad, J., Christie, G. and Dokland, T. (2011). The *Staphylococcus aureus* Pathogenicity Island 1 Protein gp6

Functions as an Internal Scaffold during Capsid Size Determination. *Journal of Molecular Biology*, 412(4), pp.710-722.

Dokland, T. (1999). Scaffolding proteins and their role in viral assembly. *Cellular and Molecular Life Sciences (CMLS)*, 56(7-8), pp.580-603.

Dyer, D., Rock, M., Yen Lee, C. and landolo, J. (1985). Generation of Transducing Particles in *Staphylococcus aureus*. *Journal of Bacteriology*, 161(1), pp.91-95.

Gibson, D. (2011). Enzymatic Assembly of Overlapping DNA Fragments. *Methods in Enzymology*, 498, pp.349-361.

Gordon, R. and Lowy, F. (2008). Pathogenesis of Methicillin-Resistant *Staphylococcus aureus* Infection. *Clinical Infectious Diseases*, 46(S5), pp.S350-S359.

Jevons, M. (1961). "Celbenin"-resistant Staphylococci. *BMJ*, 1(5219), pp.113-114.

Johnson, J. (2010). Virus particle maturation: insights into elegantly programmed nanomachines. *Current Opinion in Structural Biology*, 20(2), pp.210-216.

Karimova, G., Ullmann, A. and Ladant, D. (2000). A Bacterial Two-Hybrid System that Exploits a cAMP Signaling Cascade in *Escherichia coli*. *Methods in Enzymology*, 328, pp.59-73.

Knox, J., Uhlemann, A. and Lowy, F. (2015). *Staphylococcus aureus* infections: transmission within households and the community. *Trends in Microbiology*.

Kreiswirth, Barry N. et al. 'The Toxic Shock Syndrome Exotoxin Structural Gene Is Not Detectably Transmitted By A Prophage'. *Nature* 305.5936 (1983): 709-712. Web.

Lowy, F. (2003). Antimicrobial resistance: the example of *Staphylococcus aureus*. *Journal of Clinical Investigation*, 111(9), pp.1265-1273.

Nickoloff, J.A., editor. (1995). *Methods of Microbiology*, volume 47. Totowa, NJ; Humana Press Inc.

Novick, R. 'Properties Of A Cryptic High-Frequency Transducing Phage In *Staphylococcus Aureus*'. *Virology* 33.1 (1967): 155-166. Web.

Novick, R.P. (1991). Genetic systems in staphylococci. *Methods Enzymol* 204, 587-636.

Novick, R. (2003). Mobile genetic elements and bacterial toxinoses: the superantigen-encoding pathogenicity islands of *Staphylococcus aureus*. *Plasmid*, 49(2), pp.93-105.

Novick, R., Christie, G. and Penadés, J. (2010). The phage-related chromosomal islands of Gram-positive bacteria. *Nat Rev Micro*, 8(8), pp.541-551.

Poliakov, A., Chang, J., Spilman, M., Damle, P., Christie, G., Mobley, J. and Dokland, T. (2008). Capsid Size Determination by *Staphylococcus aureus* Pathogenicity Island SaPI1 Involves Specific Incorporation of SaPI1 Proteins into Procapsids. *Journal of Molecular Biology*, 380(3), pp.465-475.

Prevelige, P. and Fane, B. (2012). Building the Machines: Scaffolding Protein Functions During Bacteriophage Morphogenesis. In: M. Rossman and V. Rao, ed., *Viral Molecular Machines*, 1st ed. New York: Springer-Verlag, pp.325-350.

Rossman, M. (2013). Structure of viruses: a short history. *Quarterly Reviews of Biophysics*, 46(2), pp.133-180.

Spilman, M., Damle, P., Dearborn, A., Rodenburg, C., Chang, J., Wall, E., Christie, G. and Dokland, T. (2012). Assembly of bacteriophage 80 $\alpha$  capsids in a *Staphylococcus aureus* expression system. *Virology*, 434(2), pp.242-250.

Spilman, M., Dearborn, A., Chang, J., Damle, P., Christie, G. and Dokland, T. (2011). A Conformational Switch Involved in Maturation of *Staphylococcus aureus* Bacteriophage 80 $\alpha$  Capsids. *Journal of Molecular Biology*, 405(3), pp.863-876.

Suhanovsky, M. and Teschke, C. (2015). Nature's favorite building block: Deciphering folding and capsid assembly of proteins with the HK97-fold. *Virology*, 479-480, pp.487-497.

Tallent, S., Langston, T., Moran, R. and Christie, G. (2007). Transducing Particles of *Staphylococcus aureus* Pathogenicity Island SaPI1 Are Comprised of Helper Phage-Encoded Proteins. *Journal of Bacteriology*, 189(20), pp.7520-7524.

Tormo-Más, M., Mir, I., Shrestha, A., Tallent, S., Campoy, S., Lasa, Í., Barbé, J., Novick, R., Christie, G. and Penadés, J. (2010). Moonlighting bacteriophage proteins derepress staphylococcal pathogenicity islands. *Nature*, 465(7299), pp.779-782.

Ubeda, C., Olivarez, N., Barry, P., Wang, H., Kong, X., Matthews, A., Tallent, S., Christie, G. and Novick, R. (2009). Specificity of staphylococcal phage and SaPI DNA packaging as revealed by integrase and terminase mutations. *Molecular Microbiology*, 72(1), pp.98-108.

Wall, E., Caufield, J., Lyons, C., Manning, K., Dokland, T. and Christie, G. (2014). Specific N-terminal cleavage of ribosomal protein L27 in *Staphylococcus aureus* and related bacteria. *Molecular Microbiology*, 95(2), pp.258-269.

Willey, J., Sherwood, L. and Woolverton, C. (2014). *Prescott's Microbiology*. 9th ed. New York: McGraw -Hill, pp.382-383.

Xia, J., Gao, J., Kokudo, N., Hasegawa, K. and Tang, W. (2013). Methicillin-resistant *Staphylococcus aureus* antibiotic resistance and virulence. *Biosci Trends*, 7(3), pp.113-121.

## Vita

Laura Ann Klenow (*née* Waltham) was born on June 6, in Washington, D.C. She is a citizen of the United States of America. She graduated from Virginia Polytechnic Institute and State University with a Bachelor of Science in Biological Sciences. She earned a Master of Science degree in Microbiology and Immunology in 2015 from Virginia Commonwealth University.